Spike-specific CXCR3^{+} T_{FH} cells play a dominant functional role in supporting antibody responses in SARS-CoV-2 infection and vaccination

Jian Zhang[1, 2, #], Rongzhang He[1, 2, #], Bo Liu[1, #], Xingyu Zheng[1, #], Qian Wu[1, 3, #], Bo Wen[4, #], Qijie Wang[5, #], Ziyan Liu[6], Fangfang Chang[3], Yabin Hu[1], Ting Xie[5], Yongchen Liu[3], Jun Chen[7], Jing Yang[8], Shishan Teng[1], Tingting Bai[9], Yanxi Peng[10], Ze Liu[11], Yuan Peng[12], Weijin Huang[13], Velislava Terzieva[14], Youchun Wang[13, *], Wenpei Liu[1,8, 9 *,] Yi-Ping Li[3, *], Xiaowang Qu[1, 2, 7, *]

[1]Translational Medicine Institute, The First People's Hospital of Chenzhou, Hengyang Medical School, University of South China, Chenzhou, 423000, China

[2]The First School of Clinical Medicine, Xiangnan University, Chenzhou, 423000, China

[3]Institute of Human Virology, Zhongshan School of Medicine, and Key Laboratory of Tropical Disease Control of Ministry of Education, Sun Yat-sen University, Guangzhou 501180, China

[4]Department of Clinical Laboratory, Shenzhen People's Hospital, Shenzhen, 518020, China

[5]The Central Hospital of Shaoyang, Shaoyang, 422000, China

[6] The Maternal and Child Health Hospital of Hunan Province, Changsha, 410000, China

[7]School of Public Health, Southern Medical University, Guangzhou, 510515, China

[8]School of Laboratory Medicine and Biotechnology, Southern Medical University, Guangzhou, 510515, China

[9]The First School of Clinical Medicine, Southern Medical University, Guangzhou, 510515, China

[10]College of Basic Medicine, Xiangnan Univesity, Chenzhou, 423000, China

[11]School of Nursing, Xiangnan University, Chenzhou, 423000, China

[12]College of Animal Science and Technology, Guangxi University, Nanning, 530004, China

[13] National Institutes for Food and Drug Control, Key Laboratory of the Ministry of Health for Research on Quality and Standardization of Biotech Products, Key Laboratory of Biological Product Quality Research and Evaluation of National Medical Products Administration, Beijing, 102629, China

[14]Department of Clinical Immunology, University Hospital Lozenetz, Sofia, 1407, Bulgaria

[#] These authors contributed equally to this study.

[*] Corresponding authors

Correspondence should be addressed to

Xiaowang Qu, Professor

Translational Medicine Institute, The First People's Hospital of Chenzhou, Hengyang Medical School, University of South China, Chenzhou, 423000, China

Email: quxiaowang@163.com

ORCID: 0000-0002-8135-7292

Yi-Ping Li, Professor

Institute of Human Virology, Zhongshan School of Medicine, and Key Laboratory of Tropical Disease Control of Ministry of Education, Sun Yat-sen University, Guangzhou 501180, China

Email: lyiping@mail.sysu.edu.cn

ORCID: 0000-0001-6011-3101

Wenpei Liu, Associate Professor

Translational Medicine Institute, The First People's Hospital of Chenzhou, Hengyang Medical School, University of South China, Chenzhou, 423000, China

Email: wenpeiliu_2008@foxmail.com

ORCID: 0000-0002-4624-2879

Youchun Wang, Professor

National Institutes for Food and Drug Control, Key Laboratory of the Ministry of Health for Research on Quality and Standardization of Biotech Products, Key Laboratory of Biological Product Quality Research and Evaluation of National Medical Products Administration, Beijing 102629, China

Email: wangyc@nifdc.org.cn

ORCID: 0000-0001-9769-5141

Keywords: COVID-19, T follicular helper cell, C-X-C Motif Chemokine Receptor 3, Neutralizing antibody, Inactivated Vaccine

Running title: Spike-specific $CXCR3^+$ T_{FH} cells play a dominant role in supporting the antibody response

Summary

$CD4^+$ T follicular helper (T_{FH}) cells are required for high-quality antibody generation and maintenance. However, the longevity and functional role of these cells are poorly defined in COVID-19 convalescents and vaccine recipients. Here, we longitudinally investigated the dynamics and functional roles of spike-specific circulating T_{FH} cells and their subsets in convalescents at the 2^{nd}, 5^{th}, 8^{th}, 12^{th} and 24^{th} months after COVID-19 symptom onset and in vaccinees after two and three doses of inactivated vaccine. SARS-CoV-2 infection elicited robust spike-specific T_{FH} cell and antibody responses, of which spike-specific $CXCR3^+$ T_{FH} cells but not spike-specific $CXCR3^-$ T_{FH} cells and neutralizing antibodies were persistent for at least two years in more than 80% of convalescents who experienced symptomatic COVID-19, which was well coordinated between spike-specific T_{FH} cell and antibody responses at the 5^{th} month after infection. Inactivated vaccine immunization also induced spike-specific T_{FH} cell and antibody responses; however, these responses rapidly declined after six months with a two-dose standard administration, and a third dose significantly promoted antibody maturation and potency. Functionally, spike-specific $CXCR3^+$ T_{FH} cells exhibited better responsiveness than spike-specific $CXCR3^-$ T_{FH} cells upon spike protein stimulation in vitro and showed superior capacity in supporting spike-specific antibody secreting cell (ASC) differentiation and antibody production than spike-specific $CXCR3^-$ T_{FH} cells cocultured with autologous memory B cells. In conclusion, spike-specific $CXCR3^+$ T_{FH} cells played a dominant functional role in antibody elicitation and maintenance in SARS-CoV-2 infection and vaccination, suggesting that induction of CXCR3-biased spike-specific T_{FH} cell differentiation will

benefit SARS-CoV-2 vaccine development aiming to induce long-term protective immune memory.

Highlights

- SARS-CoV-2 infection elicited robust spike-specific T_{FH} cell and antibody responses, which persisted for at least two years in the majority of symptomatic COVID-19 convalescent patients.

- Inactivated vaccine immunization also elicited spike-specific T_{FH} cell and antibody responses, which rapidly declined over time, and a third dose significantly promoted antibody maturation and potency.

- Spike-specific CXCR3^{+} T_{FH} cells exhibited more durable responses than spike-specific CXCR3^{-} T_{FH} cells, correlated with antibody responses and showed superior capacity in supporting ASC differentiation and antibody production than spike-specific CXCR3^{-} T_{FH} cells.

Introduction

Severe acute respiratory syndrome coronavirus 2 (SARS-CoV-2) is the causative agent of coronavirus disease 2019 (COVID-19), which has posed a serious health threat and considerable socioeconomic consequences to the world population(Zhou et al., 2020; Zhu et al., 2020). Effective strategies are urgently needed to establish persistent and appropriate magnitude immune memory at the individual and population levels to prevent the continued spread of infection. Thus, understanding the successful immune memory in COVID-19-recovered and vaccinated individuals is essential for vaccine design to elicit long-lasting humoral and cellular immune responses against SARS-CoV-2 and variants of concern (VOCs).

Both SARS-CoV-2 natural infection and vaccination have been reported to be able to elicit robust humoral and cellular immune responses(Long et al., 2020; Meckiff et al., 2020; Mudd et al., 2022; Painter et al., 2021; Peng et al., 2020; Rydyznski Moderbacher et al., 2020; Sekine et al., 2020; Thevarajan et al., 2020; Weiskopf et al., 2020). Although immune memory has also been shown to demonstrate relatively stable B and T-cell memory in the observation period, the antibody levels are found to be waning out over time(Ibarrondo et al., 2020; Long *et al.*, 2020; Roltgen and Boyd, 2021). The early appearance of neutralizing antibodies (nAbs) associated with less severe disease in acute COVID-19 and the persistence of nAbs in recovered individuals contribute to preventing reinfection by blocking virus entry(Dupont et al., 2021; Zhou et al., 2021). To date, it is believed that reinfection of endemic human coronaviruses (HCoV-229E, HCoV-OC43, HCoV-NL63, and HCoV-HKU1) occurs frequently, primarily due to the short-lived immunoglobins induced by the endemic coronaviruses(Edridge et al., 2020). In contrast,

three highly pathogenic coronaviruses (SARS-CoV-1, MERS-CoV, and SARS-CoV-2) trigger full immune defences, eliciting stronger adaptive immunity in most recovered cases, although accumulating reinfection cases with VOCs have been reported(Cao et al., 2007; Cheon et al., 2022; Yang et al., 2022). Persistent and appropriate levels of nAbs could block virus entry, thus preventing the reinfection cycle of SARS-CoV-2 or emerging VOCs(Altmann and Boyton, 2021).

The production and maturation of high-affinity antibodies and memory B cells and long-lived plasma cell differentiation mainly rely on germinal centre (GC) reactions in secondary lymphoid tissues, which are tightly regulated by T follicular helper (T_{FH}) cells(Crotty, 2019). T_{FH} cells are specialized B helper cells that enable the proliferation, survival, and differentiation of GC B cells through the delivery of costimulatory molecules and cytokine signals(Johnston et al., 2009; Nurieva et al., 2009; Schaerli et al., 2000; Yu et al., 2009). Circulating T_{FH} cells could serve as counterparts of GC T_{FH} cells, as they express low levels of PD-1, ICOS, and Bcl6 and exhibit a memory phenotype(Morita et al., 2011). These characteristics have been correlated with high-affinity antibody responses during virus infection and vaccination(Bentebibel et al., 2016; Bentebibel et al., 2013; Martin-Gayo et al., 2017; Niessl et al., 2020; Zhang et al., 2019).

In the acute phase of SARS-CoV-2 infection, large amounts but low-affinity antibodies were produced rapidly, and in parallel, antigen-specific $CD4^+$ T cells and circulating T_{FH} cells appeared, which in turn contributed to antibody production to combat infection(Chen et al., 2020; Le Bert et al., 2020; Meckiff *et al.*, 2020; Zhou *et al.*, 2021). In COVID-19 convalescents, we and others have previously demonstrated that $CXCR3^+$ T_{FH} cells directly correlate with anti-spike antibody responses(Gong et al., 2020; Juno et

al., 2020; Zhang et al., 2021). Several studies also show that $CCR6^+$ T_{FH} cells (most are $CXCR3^-$ T_{FH} cells) were dominant and could be maintained longer after recovery in the observation period(Dan et al., 2021; Juno *et al.*, 2020; Rodda et al., 2021; Rydyznski Moderbacher *et al.*, 2020). However, the longevity and functional role of these cells in antibody elicitation and maintenance are not clear. Vaccination with the mRNA vaccine elicited strong as well as COVID-19 convalescent-specific humoral immunity, including circulating T_{FH} cell responses(Painter *et al.*, 2021; Sahin et al., 2021). More recently, several studies have shown that SARS-CoV-2 infection and mRNA vaccination efficiently induce robust GC reactions, GC-resident T_{FH} and B-cell responses, and long-lived plasma cells in bone marrow(Kim et al., 2022; Laidlaw and Ellebedy, 2022; Lederer et al., 2022; Turner et al., 2021a; Turner et al., 2021b). These responses ensure antibody production to prevent reinfection or maintain the level of circulating antibody. Although severely impaired GC reactions were found in critically ill patients or dying patients, the majority of infected or vaccinated individuals were reported to have GC reactions in lymphoid tissues for several months, which may support the maturation and maintenance of high-affinity antibodies(Duan et al., 2020; Kaneko et al., 2020; Laidlaw and Ellebedy, 2022; Poon et al., 2021; Turner *et al.*, 2021a). Nevertheless, addressing the longevity of antibody and T_{FH} cell responses as well as the functional role of T_{FH} cells in supporting the antibody response in COVID-19 convalescents and vaccinated subjects is urgently required to guide vaccine development.

In this study, we longitudinally investigated the kinetics and longevity of spike-specific antibody and T_{FH} cell responses in SARS-CoV-2 infection and vaccination and addressed the functional roles of spike-specific circulating T_{FH} cells and their subsets in supporting

ASC differentiation and antibody production. Our findings provide new insights into the development of interventions and vaccines against SARS-CoV-2 and VOCs.

Results

Persistence of spike-specific circulating T_{FH} cell responses in COVID-19 convalescents for at least 12 months

To longitudinally assess circulating T_{FH} cell and antibody responses after recovery from COVID-19, 104 blood samples were collected from 37 convalescents at the 2^{nd}, 5^{th}, 8^{th}, 12^{th}, and 24^{th} months after COVID-19 symptom onset (Figure 1A and Supporting Table 1), and PBMCs were isolated and cultured for 24 h with the stimulation of SARS-CoV-2 spike protein or BSA (5 μg/ml). Negative control PBMCs were collected from 17 healthy individuals before the COVID-19 pandemic and stimulated with the same conditions (Figure. 1B). Circulating T_{FH} ($CXCR5^+$ $CD4^+$ T) cells were gated, and a CD154 (CD40 L) assay was applied to measure antigen-specific T cells (Supporting Figure 1). The results showed that the frequencies of $CD154^+$ T_{FH} cells at the 2^{nd}, 5^{th}, 8^{th} and 12^{th} months, but not at the 24^{th} month, were significantly higher in the spike-stimulated group than in the BSA group; healthy PMBCs showed no difference in either stimulation (Figure 1B-C). These results suggest that SARS-CoV-2 infection induced spike-specific T_{FH} cell responses, which could last for at least 12 months after recovery. We also analysed spike-specific non-T_{FH} ($CXCR5^-$ $CD4^+$ T) cell responses and showed that these spike-responsive cells exhibited a similar pattern to that of T_{FH} cells maintained for at least 12 months (Supporting Figure 2A). Longitudinal analysis revealed that the frequencies of spike-specific T_{FH} cells markedly declined from the 2^{nd} to the 5^{th} month and then remained at a similar level for up to 24 months. The responsiveness capacity presented as the stimulation index (SI: spike-responsive versus BSA-responsive [baseline]) was relatively stable at each time point (Figure 1D). The kinetics of spike-specific non-T_{FH}

cells resembled those of spike-specific T_{FH} cells; however, the spike-specific non-T_{FH} cell responsiveness capacity declined significantly from the 2nd to the 5th months (SI of the 2nd month and later time points; Supporting Figure 2B). These findings suggest that SARS-CoV-2 infection elicited robust spike-specific T_{FH} cell and non-T_{FH} cell responses, of which responsiveness could be maintained for at least one year.

Spike-specific but distinct recall responses of CXCR3$^+$ and CXCR3$^-$ T_{FH} cells in COVID-19 convalescents

Previously, cross-section studies showed that the frequencies of CXCR3$^+$ T_{FH} cells or T_H1-like T_{FH} (T_{FH}1) cells were correlated with spike-specific antibody responses in COVID-19 convalescents(Boppana et al., 2021; Gong *et al.*, 2020; Juno *et al.*, 2020; Zhang *et al.*, 2021). To explore the kinetics and longevity of T_{FH} cell subset responses (Supporting Figure 1), stimulated PBMCs were further gated into CXCR3$^+$ and CXCR3$^-$ T_{FH} cell subsets, followed by analysis of CD154 expression. The results showed that CD154$^+$ CXCR3$^+$ T_{FH} cells from the 2nd to the 24th month were significantly enhanced after spike stimulation compared with BSA stimulation, while spike-responsive CXCR3$^-$ T_{FH} cells were only observed for those from the 2nd to the 8th month, and no significant changes were observed for the cells from the 12th to the 24th month (Figure 2A-B). Longitudinally, both the frequencies of spike-specific CXCR3$^+$ T_{FH} cells and spike-specific CXCR3$^-$ T_{FH} cells declined from the 2nd to the 5th month but remained relatively durable from the 5th to the 24th month (Figure 2C). The SIs of spike-specific CXCR3$^+$ and CXCR3$^-$ T_{FH} cells did not significantly vary throughout 24 months (Figure 2C). Of note, the proportion of spike-specific CXCR3$^-$ T_{FH} cells was higher than that of spike-specific CXCR3$^+$ T_{FH} cells at each time point, but spike-specific CXCR3$^+$ T_{FH} cells exhibited

superior responsiveness than spike-specific CXCR3$^-$ T_{FH} cells (higher SIs) at each time point upon stimulation (Figure 2D). PD-1 expression represents the active form of circulating T_{FH} cells, and it was found that PD-1$^+$ T_{FH} cells gradually declined over time after the resolution of COVID-19(Dan *et al.*, 2021). Here, we found that the frequencies of spike-specific PD-1$^+$ CXCR3$^+$ T_{FH} cells from the 2nd to the 12th month were significantly higher in the spike-stimulated group than in the BSA group, whereas the responsiveness of spike-specific PD-1$^+$ CXCR3$^-$ T_{FH} cells was only found at the 2nd month (Supporting Figure 3A-B), although spike-specific PD-1$^+$ CXCR3$^-$ T_{FH} cells had relatively higher frequencies than spike-specific PD-1$^+$ CXCR3$^+$ T_{FH} cells (Supporting Figure 3C). In addition, spike-responsive CXCR3$^+$ non-T_{FH} cells were maintained up to 12 months, while spike-specific CXCR3$^-$ non-T_{FH} cell responses were only observed to the 8th month upon spike stimulation (Supporting Figure 4A-B). The kinetic patterns of both spike-specific CXCR3$^+$ and CXCR3$^-$ non-T_{FH} cells were similar to those of spike-specific CXCR3$^+$ and CXCR3$^-$ T_{FH} cells, respectively (Supporting Figure 4C). The SIs of spike-specific CXCR3$^+$ non-T_{FH} cells were higher than those of CXCR3$^-$ non-T_{FH} cells from the 2nd to the 12th months (Supporting Figure 4D). Furthermore, spike-specific T_{FH} and non-T_{FH} cells, spike-specific CXCR3$^+$ T_{FH} and CXCR3$^+$ non-T_{FH} cells, and spike-specific CXCR3$^-$ and CXCR3$^-$ non-T_{FH} cells were highly correlated, respectively, from the 2nd to the 12th month, except at the 24th month, due to a limited sample size (Supporting Figure 5A-C), indicating that well-balanced spike-specific T_{FH} cell and non-T_{FH} cell responses were elicited in SARS-CoV-2 infection. Together, these data demonstrated that spike-specific CXCR3$^+$ and CXCR3$^-$ T_{FH} cells exhibited distinct recall

responses, and spike-specific CXCR3^{+} T_{FH} cells maintained a longer active state and better responsiveness than spike-specific CXCR3^{-} T_{FH} cells in COVID-19 convalescents.

Dynamics of spike-specific antibody responses in COVID-19 convalescents and correlations with T_{FH} cells

Next, to assess the kinetics of antibody responses in COVID-19 convalescents, we examined spike-specific antibodies in plasma at the 2nd, 5th, 8th, 12th and 24th months. The endpoint titer and avidity of spike-specific antibodies were determined, such as immunoglobin A (IgA), IgG and subclasses (IgG1, IgG2, and IgG3). Endpoint titers of spike-specific IgG, IgG1, IgG3, and IgA were detectable at each time point, but all declined significantly from the 2nd to the 5th month and then remained stable from the 5th to the 24th month (Figure 3A). However, spike-specific IgG2 was at a low level or undetectable at each time point (data not shown). IgA has been reported to rapidly decline, and most are short-lived(Sterlin et al., 2021). Here, IgA was found to persist for at least 24 months in symptomatic convalescents. In contrast, the avidity of the spike-specific IgG, IgG1, IgG3, and IgA antibodies increased over time with different kinetics from endpoint titers, indicating that the antibody continued to mature during the convalescent phase (Figure 3B). This finding was in line with the observation in recovered SARS patients, in which antibody avidity continued to mature from low avidity in early phase to high avidity at late phase of disease recovery(Chan et al., 2005). The maturation of antibody avidity also reflected the persistence of GC reactions after SARS-CoV-2 resolution(Poon *et al.*, 2021).

Then, we examined the neutralization activity of a plasma antibody against SARS-CoV-2 spike pseudotyped virus. The neutralization titers significantly decreased from the 2nd to

the 5th month and then gradually declined from the 5th to the 24th month (Figure 3C). Within the first 8 months, all individuals showed neutralizing antibody titers above the cut-off value (≥30); however, the titers declined, and 83% (20 out of 24) and 80% (4 out of 5) were maintained until the 12th and 24th months, respectively (Figure 3C). These data suggest that the neutralizing antibody dropped in the early phase of recovery, but the majority was maintained at a lower level for at least two years, which has similar patterns to the dynamics of the antibody endpoint titers (Figure 3A). The neutralization titers were positively associated with the endpoint titers of IgG, IgG1, IgG3, and IgA from the 2nd to the 12th month; less significant correlations were found at the 24th month, which included only five samples (Supporting Figure 6A-D). These results suggest that both IgG and IgA titers were persistent and contributed to the neutralization effect for at least two years in the majority of convalescents.

The dynamics of spike-specific T_{FH} cells and their subsets and antibody titers all declined but shared a similar pattern from the 5th to the 24th month (Figure 1-2, Figure 3A and 3C). Thus, the correlations of spike-specific T_{FH} cells or their subsets and antibody titers at each time point were further analysed. The endpoint titers of IgG1 were positively correlated with the frequencies of CD154^{+} PD-1^{+} T_{FH} and CD154^{+} PD-1^{+} CXCR3^{+} T_{FH} cells but not CD154^{+} PD-1^{+} CXCR3^{-} T_{FH} cells, and notably, these correlations were only observed at the 5th month (Figure 3D). No correlations were found between the IgG1 antibody titer and resting T_{FH} cells or their subset or non-T_{FH} cells or their subset at each time point (Supporting Figure 7A-F). Together, these results further demonstrated the potential role of spike-specific CXCR3^{+} T_{FH} cells in assisting antibody elicitation and maintenance in COVID-19.

Longitudinal analysis of spike-specific T_{FH} cell and antibody responses in inactivated vaccine recipients

SARS-CoV-2 infection elicited robust and highly correlated antibody and T_{FH} cell responses, and such responses were maintained for up to two years. To assess the dynamics of neutralizing antibodies and T_{FH} cells following vaccination, we recruited 26 participants who completed the standard vaccination procedure of the two-dose inactivated vaccine and collected blood samples from multiple time points to analyse the antibody titers and T_{FH} cell responses (Figure 4A and Supporting Table 2). The neutralization antibody reached the peak titer 14 days after the second dose of vaccination (45 days after the first dose), and then the titers rapidly decreased to a lower level at Day 180 (Figure 4B). Different from neutralization kinetics, the IgG avidity index exhibited a lower level at Days 14, 28, and 45 and then reached a plateau at Day 90 through Day 180 (Figure 4C). Notably, the peak of the vaccine-derived antibody avidity index was lower than that of natural infection with SARS-CoV-2 at the 8^{th} month (natural infection peak index versus vaccination index: median, IQR: 82.00%, 72.42%–90.21% vs. 55.37%, 49.93%–61.15%). These findings suggest that a two-dose immunization with inactivated vaccine elicited a lower level of neutralizing antibody and that these antibodies were not fully mature (low avidity) compared with the natural infection of SARS-CoV-2.

Accordingly, the frequencies of spike-specific T_{FH} and $CXCR3^-$ T_{FH} cells peaked at Day 14 after the first dose, followed by a rapid decrease and then a slight elevation after the second dose (Day 28) and were maintained at this level for at least 180 days (Figure 4D). In contrast, spike-specific $CXCR3^+$ T_{FH} cells increased slowly and peaked at Day 28,

were maintained up to Day 90, and then showed a sharp decrease at Day 180 (Figure 4D). Importantly, spike-specific CXCR3$^+$ T_{FH} cells showed stronger responsiveness (higher SIs) than spike-specific CXCR3$^-$ T_{FH} cells, although spike-specific CXCR3$^-$ T_{FH} cells had higher frequencies than spike-specific CXCR3$^+$ T_{FH} cells upon BSA or spike stimulation, which was in line with natural infection (Figure 4E). Both spike-specific PD-1$^+$ CXCR3$^+$ and PD-1$^+$ CXCR3$^-$ T_{FH} cells showed similar kinetics, levels, and responsiveness to spike-specific CXCR3$^+$ T_{FH} cells and CXCR3$^-$ T_{FH} cells, respectively (Supporting Figure 8A-C). No direct correlations between the frequencies of spike-specific PD-1$^+$ T_{FH} cells or PD-1$^+$ CXCR3$^+$ T_{FH} cells and antibody titers were observed which exhibited at the 5th month in natural infection (data not shown). To explore whether there is a link between T_{FH} cells and antibody responses in inactivated vaccine recipients, we analysed the ratio of spike-specific PD-1$^+$ CXCR3$^+$/PD-1$^+$CXCR3$^-$ T_{FH} cells and found that the ratio of spike-specific PD-1$^+$ CXCR3$^+$/PD-1$^+$ CXCR3$^-$ T_{FH} cells at Day 14 after the first dose were positively correlated with the peak neutralization titers of the second dose (Day 45) (Figure 4F). These data suggest that early primed T_{FH} cells, especially spike-specific CXCR3$^+$ T_{FH} cells, contribute to antibody production in the late phase, highlighting a key role of spike-specific CXCR3$^+$ T_{FH} cells in the early activation of CD4$^+$ T cells. In addition, spike-specific non-T_{FH} cells were also induced by the inactivated vaccine, and spike-specific CXCR3$^+$ non-T_{FH} cells were superior in response to stimulation (Supporting Figure 9A-C). These results indicate that two-dose vaccination with inactivated vaccine could efficiently elicit neutralizing antibody and activate T_{FH} cell and non-T_{FH} cell responses; however, the magnitude and persistence of these immune responses were weak and short compared to natural infection.

A third dose booster augments the T_{FH} cell response and promotes spike-specific antibody potency and maturation

Because the antibody response waned significantly after 6 months with a two-dose standard regimen, a third dose booster was recommended. To test the antibody and T_{FH} cell responses before and after the third-dose vaccination, we recruited 24 individuals who had completed a two-dose regimen for at least 6 months and collected PBMCs before and 14 days after the third dose boost (Supporting Table 2). The third dose dramatically increased the neutralization titer more than 12-fold (Figure 5A) and significantly promoted antibody affinity maturation (Figure 5B), reaching a level similar to that of natural infection (natural infection peak index versus vaccination index: median, IQR: 82.00%, 72.42%–90.21% vs. 86.11%, 84.99%–88.42%). T_{FH} cells and $CXCR3^+$ and $CXCR3^-$ T_{FH} cell subsets all responded to spike stimulation before and after the third dose booster (Figure 5C); however, the expansion of spike-specific $CXCR3^+$ T_{FH} cells was apparently faster and higher than that of spike-specific $CXCR3^-$ T_{FH} cells (Figure 5D-E). Furthermore, the ratio of spike-specific $PD\text{-}1^+$ $CXCR3^+$/ $PD\text{-}1^+$ $CXCR3^-$ T_{FH} cells before the booster was significantly correlated with the neutralization titers after the booster (Figure 5F). These results suggested that the spike-specific T_{FH} cells elicited by the two-dose regimen further supported antibody production following the third dose booster. Spike-specific non-T_{FH} cells and $CXCR3^+$ and $CXCR3^-$ non-T_{FH} cell subsets were also expanded by the third dose (Supporting Figure 10A-B), but spike-specific $CXCR3^+$ non-T_{FH} cells were more efficiently expanded than spike-specific $CXCR3^-$ non-T_{FH} cells upon spike stimulation (Supporting Figure 10 C). Thus, these data showed that the third dose booster augmented the responses of antibody, spike-specific T_{FH} cells and

their subsets and non-T_{FH} cells, of which spike-specific $CXCR3^+$ T_{FH} cells were preferentially expanded and contributed to antibody quality and quantity enhancement.

Spike-specific $CXCR3^+$ T_{FH} cells from natural infection and vaccination show superior capacity than spike-specific $CXCR3^-$ T_{FH} cells in supporting antibody-secreting cell differentiation and antibody production in vitro

Previous studies have shown that both spike-specific $CD4^+$ T cells and T_{FH} cells are associated with antibody production in SARS-CoV-2 infection(Gong *et al.*, 2020; Juno *et al.*, 2020; Peng *et al.*, 2020; Reynolds et al., 2020; Zhang *et al.*, 2021). To discriminate the functional role of these cells in supporting ASC differentiation and antibody production, we cocultured T_{FH} cells or non-T_{FH} cells with autologous memory B cells (5×10^4 cells for each cell type) (Figure 6A). The T_{FH} cells or non-T_{FH} cells from each group of healthy controls, convalescents, and vaccine recipients were cocultured with autologous memory B cells for 6 days in the presence of *staphylococcal enterotoxin* B (SEB), total ASCs ($CD38^{hi}$ $CD27^{hi}$ B cells) and spike-specific ASCs were measured by FACS (Figure 6B), and spike-specific IgG was measured by ELISA (Figure 6C-F, right panel). In healthy controls, T_{FH} cells but not non-T_{FH} cells efficiently supported autologous memory B cells differentiated into total ASCs, as expected spike-specific ASCs and IgG were rarely observed (Figure 6C). T_{FH} cells from convalescents and vaccinees efficiently supported autologous memory B cells differentiated into both total ASCs and spike-specific ASCs and produced spike-specific IgG (Figure 6D-E). The third dose further enhanced the humoral immune responses, as more spike-specific ASCs and IgG were produced in comparison with before booster (Figure 6F). Moreover, the frequencies of spike-specific ASCs correlated with spike-specific IgG OD_{450} (Supporting

Figure 11). Taken together, we conclude that T_{FH} cells, but not non-T_{FH} cells, were the major player in assisting antibody production and maintenance in SARS-CoV-2 infection and vaccination, which positively correlated with antibody responses (Figure 3D and Supporting Figure 7D-F; Figure 4F and Figure 5F).

According to the results above, we found that spike-specific $CXCR3^+$ T_{FH} cells were associated with antibody magnitude and exhibited better responsiveness than spike-specific $CXCR3^-$ T_{FH} cells in both natural infection and vaccination, but the functional difference of spike-specific $CXCR3^+$ T_{FH} cells and spike-specific $CXCR3^-$ T_{FH} cells was not clear. To further discriminate the functional role of spike-specific $CXCR3^+$ T_{FH} cells and spike-specific $CXCR3^-$ T_{FH} cells in supporting ASC differentiation and antibody production. Both bulk $CXCR3^+$ and $CXCR3^-$ T_{FH} cells were sorted from COVID-19 convalescents and vaccine recipients and cocultured with autologous memory B cells (Figure 6G). $CXCR3^-$ T_{FH} cells were more efficient in supporting memory B-cell differentiation into total ASCs (Figure 6I and 6J, left panel); however, $CXCR3^+$ T_{FH} cells showed superior capacity than $CXCR3^-$ T_{FH} cells in supporting spike-specific ASC differentiation (Figure 6H; Figure 6I and 6J, middle panel), although we did not observe higher spike-specific IgG production in $CXCR3^+$ T_{FH} cells than in $CXCR3^-$ T_{FH} cells cocultured with autologous memory B cells, as expected (Figure 6I and 6J, right panel). This might be due to the lower proportions of spike-specific $CXCR3^+$ T_{FH} cells within $CXCR3^+$ T_{FH} cells than spike-specific $CXCR3^-$ T_{FH} cells within $CXCR3^-$ T_{FH} cells (Figure 2D and Figure 4E), although there was a higher responsiveness of spike-specific $CXCR3^+$ T_{FH} cells than spike-specific $CXCR3^-$ T_{FH} cells in convalescent and vaccine recipients (Figure 2D and Figure 4E). These findings further suggest that spike-specific

T_{FH} cells, especially the spike-specific $CXCR3^{+}$ subset, play a dominant role in assisting antibody production and maintenance in natural infection and vaccination.

Discussion

In this study, we systemically investigated the longitudinal dynamics of spike-specific T_{FH} cell and antibody responses in individuals up to two years after COVID-19 recovery and those who received two and three doses of inactivated vaccine. We discovered that spike-specific T_{FH} cells, especially spike-specific CXCR3$^+$ T_{FH} cells, played a dominant functional role in supporting high-quality antibody elicitation and maintenance in convalescents and inactivated vaccine recipients. Both natural infection and vaccination generated memory B cells, which could be recalled efficiently by spike-specific T_{FH} cells to differentiate into ASCs and produce spike-specific antibodies. These findings suggest that long-term humoral immunity could be generated and recalled, thus providing new insight into COVID-19 immunity and inspiring the evaluation of long-term protection.

Previous studies have shown that SARS-CoV-2 infection induces robust spike-specific T_H1 and T_{FH} cell responses in the acute phase, which are maintained in the convalescent phase and persist for several months to a year(Dan *et al.*, 2021; Marcotte et al., 2022; Rodda *et al.*, 2021). Here, in the longitudinal analysis of circulating T_{FH} cells through a 2-year period in COVID-19 convalescents, we found that spike-specific T_{FH} cells rapidly declined from the 2nd to the 5th month and then remained stable for at least 12 months. The spike-specific CXCR3$^+$ T_{FH} cell responses persisted for up to 24 months or more. Importantly, the decline in spike-specific PD-1$^+$ active T_{FH} cells may account for the constraint memory T_{FH} cells after the 5th month of recovery. In most symptomatic COVID-19 cases, robust GC reactions were demonstrated and found to be able to be maintained for at least six months(Laidlaw and Ellebedy, 2022; Poon *et al.*, 2021). GC T_{FH} cells assist B-cell maturation and differentiation into high-affinity memory B cells

and long-lived plasma cells. The long-term persistence of circulating T_{FH} cell responses may be attributed to active GC reactions in lymph nodes after recovery.

In line with the dynamics of T_{FH} cells, spike-specific IgG, IgG1, IgG3, and IgA antibody endpoint titers as well as neutralization titers showed a sharp decline from the 2nd to the 5th month and then were maintained in the majority of convalescents at the level for at least 24 months, longer than the 16 months reported recently(Yang *et al.*, 2022). The sharp decrease was most likely due to the short half-life of serum antibodies and ASCs(Dan *et al.*, 2021). ASCs normally decay within a few weeks, and only a population of long-lived plasma cells can live from several months to years(Hammarlund et al., 2017). IgA has been shown to play a dominant role in neutralization in early infection, although it is short-lived and declines rapidly after infection(Sterlin *et al.*, 2021). Here, we found that spike-specific IgA antibodies were maintained for 24 months, although at a lower level, much longer than a previous observation that IgA was detectable six months after infection, which may also contribute to long-term protection(Roltgen and Boyd, 2021). Antibody maturation is a relatively slow process that is supported by T_{FH} cells in the GC(Crotty, 2019). Our results showed that spike-specific IgG antibody maturation peaked at the 5th-8th month after infection, while spike-specific IgG3 and IgA became fully mature at the 12th month. These data indicated that long-term T_{FH} cell responses are required in COVID-19 convalescents to gradually support high-quality antibody maturation and maintenance.

Inactivated vaccines have been widely used and proven to elicit robust and broad humoral immunity by the two-dose immunization procedure, which could protect against infection from VOC infection or severe disease(Chen et al., 2022; Liu et al., 2022). In

this study, we also found that inactivated vaccine immunization mounted humoral immunity in a similar pattern to natural infection, but the magnitudes of antibody and T_{FH} cell responses were significantly lower. Although neutralizing antibody peaked at 14 days after the second dose and antibody matured at 3 months after the first dose, spike-specific T_{FH} cells could be observed at 14 days after the first dose, earlier than the appearance of neutralizing antibody. However, the neutralizing antibody significantly declined at 6 months after immunization. Based on the memory immunity generated by the two-dose injection, the third dose booster significantly magnified the neutralizing antibody titers, along with increased antibody maturation and responsive T_{FH} cells. These results were consistent with several recent studies on inactivated vaccine showing that a third-dose immunization increased the antibody neutralizing effect for SARS-CoV-2 and some VOCs, proving the enhancement and necessity of the third-dose booster(Liu *et al.*, 2022; McMenamin et al., 2022). However, the T_{FH} cell and antibody responses elicited by inactivated vaccines seem to last a short period of time, different from natural infections, which elicit a lasting and relatively stable immune memory response(Marcotte *et al.*, 2022). In addition, current intramuscular injection immunization only mounted a poor IgA response, which is important for mucosal immunity in the respiratory tract(Liu *et al.*, 2022). Together, to maintain recallable immunity, heterogonous sequential immunization may be a strategy for improving immunization efficacy, especially intranasal immunization to elicit local mucosal immunity.

The long-lived antibody response is mainly supported by T_{FH} cells in natural infection and vaccination(Laidlaw and Ellebedy, 2022; Roltgen et al., 2022). We found that SARS-CoV-2 infection and vaccination induced robust spike-specific $CD4^+$ T cells, comprising

T_H1 and T_{FH} cell responses, consistent with other studies, thus laying the foundation for long-term immunity(Chen *et al.*, 2022; Liu *et al.*, 2022). Longitudinal analysis showed that spike-specific T_{FH} and non-T_{FH} cell responses were maintained for at least 12 months and were more stable in COVID-19 convalescent than inactivated vaccine recipients, although the dynamics were similar in both cohorts. Notably, spike-specific T_{FH} cells, especially spike-specific $CXCR3^+$ T_{FH} cells, positively correlated with antibody responses at the 5^{th} month in convalescents, in which the quantity and quality of antibodies were well balanced. Although spike-specific T_{FH} cells did not correlate with the neutralizing antibody titer in the vaccine recipients, the ratio of spike-specific $CXCR3^+/CXCR3^-$ T_{FH} cells at Day 14 after the first dose, representative of T_H1-like T_{FH} cell bias, positively correlated with the neutralizing titer on Day 45 (Day 14 after the second dose). In addition, the T_{FH} cells, not non-T_{FH} cells, elicited by the two-dose immunization were associated with the antibody magnitude after the third dose. Functionally, T_{FH} cells could recall autologous memory B cells to differentiate into total ASCs, spike-specific ASCs and antibodies, but non-T_{FH} cells could not stimulate a detectable level of ASCs. Therefore, circulating spike-specific T_{FH} cells are a surrogate of bona fide GC T_{FH} cells that support spike-specific ASC differentiation and antibody production in natural infection and vaccination(Morita *et al.*, 2011). Of note, our study did not exclude the possibility that non-T_{FH} cells supported short-lived plasmablast differentiation and produced low affinity antibodies in the very early acute phase to constrain infection rapidly, as large amounts of antibodies could be produced by extrafollicular B cells in some severe cases(Woodruff et al., 2020).

SARS-CoV-2 infection-induced circulating T_{FH} cells exhibited a clear phenotypic bias towards a $CCR6^+$ $CXCR3^-$ phenotype, and these subsets comprised the large proportions of spike-specific T_{FH} cells in natural infection(Dan *et al.*, 2021; Juno *et al.*, 2020; Rodda *et al.*, 2021; Rydyznski Moderbacher *et al.*, 2020). We and others have previously shown that the $CXCR3^+$ T_{FH} cell subset is increased in convalescents and positively correlated with the spike-specific antibody response(Gong *et al.*, 2020; Juno *et al.*, 2020; Zhang *et al.*, 2021). The association of T_H1-like ($CXCR3^+$) T_{FH} cells with the quantity and quality of antibody was also characterized in influenza vaccine recipients and in other chronic viral infections(Bentebibel *et al.*, 2016; Bentebibel *et al.*, 2013; Koutsakos et al., 2018; Niessl *et al.*, 2020; Zhang *et al.*, 2019). Furthermore, we have demonstrated that $CXCR3^+$ and $CXCR3^-$ T_{FH} subsets have distinct phenotypes and functions in HCV infection(Zhang *et al.*, 2019). Here, spike-specific $CXCR3^+$ T_{FH} cells showed an active status and maintained responsiveness for a longer time than spike-specific $CXCR3^-$ T_{FH} cells in convalescents. However, the functional significance of $CXCR3^+$ T_{FH} cells in SARS-CoV-2 infection and vaccination is extremely unknown. Coculture of $CXCR3^+$ T_{FH} or $CXCR3^-$ T_{FH} cells with autologous memory B cells from COVID-19 convalescents and vaccinees showed that $CXCR3^+$ T_{FH} cells exhibited superior capacity than $CXCR3^-$ T_{FH} cells in supporting spike-specific memory B cells differentiated into ASCs, confirming that spike-specific $CXCR3^+$ T_{FH} cells played a dominant function in assisting the antibody response in natural infection and vaccination, although the proportions of spike-specific $CXCR3^+$ T_{FH} cells were lower than those of $CXCR3^-$ T_{FH} cells.

The T_H1-polarizing conditions of a viral infection usually result in the predominant generation of T_H1-like T_{FH} cells, such as influenza vaccination, following live-attenuated

yellow fever vaccination and HCV and Zika virus infection(Bentebibel *et al.*, 2016; Bentebibel *et al.*, 2013; Liang et al., 2019; Martin-Gayo *et al.*, 2017; Zhang *et al.*, 2019). Given the importance of T_H1-like T_{FH} cells in supporting the production of high-quality antibodies and the longevity of secreting cells, strategies to promote T_H1-like T_{FH} cell polarization would benefit SARS-CoV-2 vaccine improvement. In this study, we found that spike-specific $CXCR3^+$ T_{FH} cells show long-term persistence and play a dominant role in supporting the antibody response. These findings will inform vaccine design towards long-term protection against SARS-CoV-2 infection.

Materials and Methods

Study subjects This study included two cohorts, convalescents and vaccinated subjects. Thirty-seven COVID-19 convalescent subjects were from The Central Hospital of Shaoyang, Hunan Province, China, and all were followed up to 24 months after symptom onset (Supporting Table 1). Another 37 vaccinated subjects were from The First People's Hospital of Chenzhou, Hunan Province, China. All received two doses of inactivated vaccine (Sinovac, China), and 24 received the third-dose vaccination (Supporting Table 2). Each participant signed a written consent form. The study protocol was approved by the Institutional Ethical Review Board of The Central Hospital of Shaoyang (V.1.0, 20200301) and the First People's Hospital of Chenzhou (V.3.0, 2021001). Blood samples of COVID-19 convalescents were collected at the 2^{nd}, 5^{th}, 8^{th}, 12^{th} and 24^{th} months after COVID-19 symptom onset. Blood samples of vaccine recipients were collected before vaccination and 14, 28, 45, 90, and 180 days after inoculation with the first dose; blood samples from 24 recipients were taken before and 14 days after the third dose vaccination (Supporting Table 1 & Table 2). Seventeen healthy individuals before the COVID-19 pandemic were used as the negative control. PBMCs and plasma were isolated and stored in liquid nitrogen in a -80 °C freezer.

Endpoint titer of antibody

The endpoint titers of spike-specific antibodies were determined by measuring the binding activity of serially diluted plasma to the SARS-CoV-2 spike protein using ELISA. In brief, 96-well plates (Corning, NY, USA) were coated with SARS-CoV-2 spike protein (SARS-CoV-2 S1+S2_ECD, 200 ng/well) (Sino Biological, Beijing, China) in PBS and incubated at 4 °C overnight. The plates were washed five times with PBS-T

(0.05% Tween-20 in PBS) and then blocked with blocking buffer (2% FBS and 2% BSA in PBS-T) for 30 min. Two-fold serial dilutions of plasma, starting from a 1:20 dilution, were added to the 96-well plates in triplicate (100 µl/well) and incubated for 1 h at room temperature. Spike-specific antibodies were detected using horseradish peroxidase (HRP)-conjugated anti-human IgG (Jackson ImmunoResearch, PA, USA), IgG1, IgG3 (BaiaoTong Experiment Center, Luoyang, China), and IgA (Thermo Fisher Scientific, Waltham, MA, USA). Plasma from healthy subjects was collected before the COVID-19 pandemic as a negative control, and SARS-CoV-2 spike RBD-specific monoclonal antibody was generated in the laboratory and used as a positive control. Optical density at 450 nm (OD_{450}) was measured for each reaction, and an OD_{450} of three-fold above the cut-off value was considered a positive readout. The highest dilution showing a positive readout was defined as the endpoint titer of the antibody, and the data were logarithmically transformed.

Antibody avidity assay

The avidity of spike-specific antibodies (IgG, IgG1, IgG3 and IgA) was measured using a modified 2-step approach that we described previously(Zhang *et al.*, 2021). In the first step, plasma dilutions were optimized to obtain an OD_{450} value within the range of 0.5-1.5 to ensure a linear measurement of the antibody avidity. The second step was an ELISA but included an elution procedure of 1 M NaSCN. These measurements were performed in triplicate. The avidity index of an antibody was calculated as $OD_{NaSCN\ 1M}/OD_{NaSCN\ 0M} \times 100\%$.

Antibody neutralization assay

The neutralization activity of plasma was determined by the reduction in luciferase expression after pseudotyped virus infection of Huh7 cells, as described previously(Zhang *et al.*, 2021). In brief, SARS-CoV-2 pseudotyped virus was incubated in duplicate with serial dilutions of plasma samples (six dilutions: 1:30; 1:90; 1:270; 1:810; 1:2430; 1:7290) at 37 °C for 1h. Then, freshly trypsinized cells were added at 5% CO_2 and incubated at 37 °C for 24 h, and the luminescence was measured. In parallel, control wells with virus only or cells only were included in six replicates. The background relative light unit (RLU) (wells with cells only) was subtracted from each determination. Plasma from healthy controls was used as a negative control. Plasma from guinea pigs immunized with the SARS-CoV-2 spike protein was used as a positive control. The 50% inhibitory dilution (ID_{50}) was defined as the plasma dilution, of which the RLU was reduced by 50% compared with the control solution wells (virus + cells). The cut-off value was defined as ID_{50}=30, and ID_{50}>30 was considered to have a neutralization effect.

Antigen-specific T_{FH} cell assay

To analyse spike-specific T_{FH} cells, a CD154 (CD40 L) assay was used to assess the response of circulating T_{FH} cells upon stimulation. In brief, cryopreserved PBMCs were thawed and allowed to recover in complete RPMI 1640 medium in 5% CO_2 at 37 °C overnight. PBMCs (1×10^6) were stimulated with SARS-CoV-2 spike protein (S1+S2_ECD, 5 μg/ml, Sino Biological, Beijing, China) or BSA (5 μg/ml, Sigma□Aldrich, St. Louis, MO, USA) in 5% CO_2 at 37 °C for 24 h, PE mouse anti-human CD154 (24-31) (BioLegend, San Diego, CA, USA) was added during the stimulation. Concanavalin A (Con A, 5 μg/ml, Sigma□Aldrich, St. Louis, MO, USA)

was used as a positive control. In parallel, PBMCs from healthy controls were stimulated under the same conditions. After stimulation, the cells were labelled with a LIVE/DEAD® Fixable Blue Dead Cell Stain Kit (Thermo Fisher Scientific, Waltham, MA, USA) to distinguish dead cells and then treated with Fc Block (BioLegend, San Diego, CA, USA) to block nonspecific binding. The treated PBMCs were stained with antibodies that had been pretitrated to an optimized dilution and fluorescently labelled in 96-well V-bottom plates at 4 °C for 30 min. The fluorescent labelled antibodies were BUV737 mouse anti-human CD4 (SK3), PE mouse anti-human CXCR3 (1C6) (BD Biosciences, Franklin Lake, NJ, USA), FITC mouse anti-human PD-1 (EH12.2H7) (BioLegend, San Diego, CA, USA), and PE-eFluor 610 mouse anti-human CXCR5 (MU5UBEE) (Thermo Fisher Scientific, Waltham, MA, USA). Samples were loaded onto a MoFlo XDP Flow Cytometer (Beckman Coulter, Brea, CA, USA) immediately after antibody staining. The cells were gated with the strategy (Supporting Figure 1) as spike-specific T_{FH} cells ($CD154^+$ $CXCR5^+$ $CD4^+$ T cells), spike-specific $CXCR3^+$ T_{FH} cells ($CD154^+$ $CXCR3^+$ $CXCR5^+$ $CD4^+$ T cells), spike-specific $CXCR3^-$ T_{FH} cells ($CD154^+$ $CXCR3^-$ $CXCR5^+$ $CD4^+$ T cells), active T_{FH} cells ($CD154^+$ $PD\text{-}1^+$ $CXCR5^+$ $CD4^+$ T cells), and spike-specific non-T_{FH} cells ($CD154^+$ $CXCR5^-$ $CD4^+$ T cells). The responsiveness capacity presented as the stimulation index (SI: spike-responsive versus BSA-responsive [baseline]). The gating of cell populations was based on the mean fluorescence intensity “minus one” (FMO) and unstained control. All data were analysed using FlowJo 10.0 software (Tree Star, San Carlos, CA, USA).

T_{FH} and memory B-cell coculture

To test the functional role of T_{FH} cells, $CXCR3^+$ and $CXCR3^-$ T_{FH} cell subsets, and non-

T_{FH} cells in supporting ASC differentiation and antibody production, these cells were cocultured with autologous memory B cells. In detail, $CD4^+$ T cells and $CD19^+$ B cells were primarily sorted from PBMCs of convalescents and vaccinees by CD4 and CD19 MicroBeads (Miltenyi Biotec, Bergisch Gladbach, Germany), respectively. Purified $CD4^+$ T cells and $CD19^+$ B cells were sorted into T_{FH} cells ($CXCR5^+$ $CD4^+$ T cells), non-T_{FH} cells ($CXCR5^-$ $CD4^+$ T cells), $CXCR3^+$ T_{FH} cells ($CXCR3^+$ $CXCR5^+$ $CD4^+$ T cells), $CXCR3^-$ T_{FH} cells ($CXCR3^-$ $CXCR5^+$ $CD4^+$ T cells), and memory B cells ($CD20^+$ $CD27^+$ B cells) by FACS. $CD4^+$ T cells were labelled with a LIVE/DEAD® Fixable Blue Dead Cell Stain Kit (Thermo Fisher Scientific, Waltham, MA, USA) to distinguish dead cells in a 15 ml centrifuge tube at 4 °C for 30 min and then stained with BUV737 mouse anti-human CD4 (SK3), PE mouse anti-human CXCR3 (1C6) (BD Biosciences, Franklin Lake, NJ, USA), and PE-eFluor 610 mouse anti-human CXCR5 (MU5UBEE) (Thermo Fisher Scientific, Waltham, MA, USA). $CD19^+$ B cells were stained with mouse anti-human CD20 PE (2H7), mouse anti-human PE-Cy™7 CD27 (M-T271) (BioLegend, San Diego, CA, USA). Sorted T_{FH}, non-T_{FH}, $CXCR3^+$ T_{FH}, and $CXCR3^-$ T_{FH} cells (5×10^4 cells for each type) were cocultured with autologous memory B cells (5×10^4 cells) in the presence of 100 ng/ml *staphylococcal enterotoxin* B (SEB) (Toxin Technology, Sarasota, FL, USA) and RPMI 1640 medium supplemented with 10% FBS in 96-well U-bottom plates for 6 days. After coculture, spike-specific IgG in the supernatant was determined by ELISA. Antibody-secreting cells (ASCs) ($CD4^-$ $CD27^{hi}$ $CD38^{hi}$ cells) and spike-specific ASCs (spike-probe $FITC^+$ and spike-probe $ALEX647^+$ $CD4^-$ $CD27^{hi}$ $CD38^{hi}$ cells) were analysed by flow cytometry. Spike-specific ASCs were intracellularly stained. All data analyses were performed with FlowJo 10.0 software (Tree Star, San Carlos, CA,

USA).

Statistical analysis

All data were analysed by the Kolmogorov–Smirnov test for normal distribution. When variables were nonnormally distributed, data were expressed as the median ± IQR (interquartile range), and Mann–Whitney U tests were used to analyse two independent variables. For paired sample comparison, data were expressed as each individual value or mean ± SEM (standard error of mean), and paired t tests were used to analyse the differences between two groups. Differences among multiple groups were compared with one-way analysis of variance, and Tukey's test was used between two groups at the same time point. Spearman's rank correlation coefficient was used to measure the correlation between two different variables. Analyses of the data were performed using SPSS v.26 and GraphPad Prism v.8.0. All numerical data shown in this study were collected from at least three independent experiments.

Reference

Altmann, D.M., and Boyton, R.J. (2021). Waning immunity to SARS-CoV-2: implications for vaccine booster strategies. Lancet Respir Med *9*, 1356-1358. 10.1016/S2213-2600(21)00458-6.

Bentebibel, S.E., Khurana, S., Schmitt, N., Kurup, P., Mueller, C., Obermoser, G., Palucka, A.K., Albrecht, R.A., Garcia-Sastre, A., Golding, H., and Ueno, H. (2016). ICOS(+)PD-1(+)CXCR3(+) T follicular helper cells contribute to the generation of high-avidity antibodies following influenza vaccination. Sci Rep *6*, 26494. 10.1038/srep26494.

Bentebibel, S.E., Lopez, S., Obermoser, G., Schmitt, N., Mueller, C., Harrod, C., Flano, E., Mejias, A., Albrecht, R.A., Blankenship, D., et al. (2013). Induction of ICOS+CXCR3+CXCR5+ TH cells correlates with antibody responses to influenza vaccination. Sci Transl Med *5*, 176ra132. 10.1126/scitranslmed.3005191.

Boppana, S., Qin, K., Files, J.K., Russell, R.M., Stoltz, R., Bibollet-Ruche, F., Bansal, A., Erdmann, N., Hahn, B.H., and Goepfert, P.A. (2021). SARS-CoV-2-specific circulating T follicular helper cells correlate with neutralizing antibodies and increase during early convalescence. PLoS Pathog *17*, e1009761. 10.1371/journal.ppat.1009761.

Cao, W.C., Liu, W., Zhang, P.H., Zhang, F., and Richardus, J.H. (2007). Disappearance of antibodies to SARS-associated coronavirus after recovery. N Engl J Med *357*, 1162-1163. 10.1056/NEJMc070348.

Chan, P.K., Lim, P.L., Liu, E.Y., Cheung, J.L., Leung, D.T., and Sung, J.J. (2005). Antibody avidity maturation during severe acute respiratory syndrome-associated coronavirus infection. J Infect Dis *192*, 166-169. 10.1086/430615.

Chen, G., Wu, D., Guo, W., Cao, Y., Huang, D., Wang, H., Wang, T., Zhang, X., Chen, H., Yu, H., et al. (2020). Clinical and immunological features of severe and moderate coronavirus disease 2019. J Clin Invest *130*, 2620-2629. 10.1172/JCI137244.

Chen, Y., Yin, S., Tong, X., Tao, Y., Ni, J., Pan, J., Li, M., Wan, Y., Mao, M., Xiong, Y., et al. (2022). Dynamic SARS-CoV-2-specific B-cell and T-cell responses following immunization with an inactivated COVID-19 vaccine. Clin Microbiol Infect *28*, 410-418. 10.1016/j.cmi.2021.10.006.

Cheon, S., Park, U., Park, H., Kim, Y., Nguyen, Y.T.H., Aigerim, A., Rhee, J.Y., Choi, J.P., Park, W.B., Park, S.W., et al. (2022). Longevity of seropositivity and neutralizing antibodies in recovered MERS patients: a 5-year follow-up study. Clin Microbiol Infect *28*, 292-296. 10.1016/j.cmi.2021.06.009.

Crotty, S. (2019). T Follicular Helper Cell Biology: A Decade of Discovery and Diseases. Immunity *50*, 1132-1148. 10.1016/j.immuni.2019.04.011.

Dan, J.M., Mateus, J., Kato, Y., Hastie, K.M., Yu, E.D., Faliti, C.E., Grifoni, A., Ramirez, S.I., Haupt, S., Frazier, A., et al. (2021). Immunological memory to SARS-CoV-2 assessed for up to 8 months after infection. Science *371*. 10.1126/science.abf4063.

Duan, Y.Q., Xia, M.H., Ren, L., Zhang, Y.F., Ao, Q.L., Xu, S.P., Kuang, D., Liu, Q., Yan, B., Zhou, Y.W., et al. (2020). Deficiency of Tfh Cells and Germinal Center in Deceased COVID-19 Patients. Curr Med Sci *40*, 618-624. 10.1007/s11596-020-2225-x.

Dupont, L., Snell, L.B., Graham, C., Seow, J., Merrick, B., Lechmere, T., Maguire, T.J.A., Hallett, S.R., Pickering, S., Charalampous, T., et al. (2021). Neutralizing antibody activity in convalescent sera from infection in humans with SARS-CoV-2 and variants of concern. Nat Microbiol *6*, 1433-1442. 10.1038/s41564-021-00974-0.

Edridge, A.W.D., Kaczorowska, J., Hoste, A.C.R., Bakker, M., Klein, M., Loens, K., Jebbink, M.F., Matser, A., Kinsella, C.M., Rueda, P., et al. (2020). Seasonal coronavirus protective immunity is short-lasting. Nat Med *26*, 1691-1693. 10.1038/s41591-020-1083-1.

Gong, F., Dai, Y., Zheng, T., Cheng, L., Zhao, D., Wang, H., Liu, M., Pei, H., Jin, T., Yu, D., and Zhou, P. (2020). Peripheral CD4+ T cell subsets and antibody response in COVID-19 convalescent individuals. J Clin Invest *130*, 6588-6599. 10.1172/JCI141054.

Hammarlund, E., Thomas, A., Amanna, I.J., Holden, L.A., Slayden, O.D., Park, B., Gao, L., and Slifka, M.K. (2017). Plasma cell survival in the absence of B cell memory. Nat Commun *8*, 1781. 10.1038/s41467-017-01901-w.

Ibarrondo, F.J., Fulcher, J.A., Goodman-Meza, D., Elliott, J., Hofmann, C., Hausner, M.A., Ferbas, K.G., Tobin, N.H., Aldrovandi, G.M., and Yang, O.O. (2020). Rapid Decay of Anti-SARS-CoV-2 Antibodies in Persons with Mild Covid-19. N Engl J Med *383*, 1085-1087. 10.1056/NEJMc2025179.

Johnston, R.J., Poholek, A.C., DiToro, D., Yusuf, I., Eto, D., Barnett, B., Dent, A.L., Craft, J., and Crotty, S. (2009). Bcl6 and Blimp-1 are reciprocal and antagonistic regulators of T follicular helper cell differentiation. Science *325*, 1006-1010. 10.1126/science.1175870.

Juno, J.A., Tan, H.X., Lee, W.S., Reynaldi, A., Kelly, H.G., Wragg, K., Esterbauer, R., Kent, H.E., Batten, C.J., Mordant, F.L., et al. (2020). Humoral and circulating follicular helper T cell responses in recovered patients with COVID-19. Nat Med *26*, 1428-1434. 10.1038/s41591-020-0995-0.

Kaneko, N., Kuo, H.H., Boucau, J., Farmer, J.R., Allard-Chamard, H., Mahajan, V.S., Piechocka-Trocha, A., Lefteri, K., Osborn, M., Bals, J., et al. (2020). Loss of Bcl-6-Expressing T Follicular

Helper Cells and Germinal Centers in COVID-19. Cell *183*, 143-157 e113. 10.1016/j.cell.2020.08.025.

Kim, W., Zhou, J.Q., Horvath, S.C., Schmitz, A.J., Sturtz, A.J., Lei, T., Liu, Z., Kalaidina, E., Thapa, M., Alsoussi, W.B., et al. (2022). Germinal centre-driven maturation of B cell response to mRNA vaccination. Nature *604*, 141-145. 10.1038/s41586-022-04527-1.

Koutsakos, M., Wheatley, A.K., Loh, L., Clemens, E.B., Sant, S., Nussing, S., Fox, A., Chung, A.W., Laurie, K.L., Hurt, A.C., et al. (2018). Circulating TFH cells, serological memory, and tissue compartmentalization shape human influenza-specific B cell immunity. Sci Transl Med *10*. 10.1126/scitranslmed.aan8405.

Laidlaw, B.J., and Ellebedy, A.H. (2022). The germinal centre B cell response to SARS-CoV-2. Nat Rev Immunol *22*, 7-18. 10.1038/s41577-021-00657-1.

Le Bert, N., Tan, A.T., Kunasegaran, K., Tham, C.Y.L., Hafezi, M., Chia, A., Chng, M.H.Y., Lin, M., Tan, N., Linster, M., et al. (2020). SARS-CoV-2-specific T cell immunity in cases of COVID-19 and SARS, and uninfected controls. Nature *584*, 457-462. 10.1038/s41586-020-2550-z.

Lederer, K., Bettini, E., Parvathaneni, K., Painter, M.M., Agarwal, D., Lundgreen, K.A., Weirick, M., Muralidharan, K., Castano, D., Goel, R.R., et al. (2022). Germinal center responses to SARS-CoV-2 mRNA vaccines in healthy and immunocompromised individuals. Cell *185*, 1008-1024 e1015. 10.1016/j.cell.2022.01.027.

Liang, H., Tang, J., Liu, Z., Liu, Y., Huang, Y., Xu, Y., Hao, P., Yin, Z., Zhong, J., Ye, L., et al. (2019). ZIKV infection induces robust Th1-like Tfh cell and long-term protective antibody responses in immunocompetent mice. Nat Commun *10*, 3859. 10.1038/s41467-019-11754-0.

Liu, Y., Zeng, Q., Deng, C., Li, M., Li, L., Liu, D., Liu, M., Ruan, X., Mei, J., Mo, R., et al. (2022). Robust induction of B cell and T cell responses by a third dose of inactivated SARS-CoV-2 vaccine. Cell Discov *8*, 10. 10.1038/s41421-022-00373-7.

Long, Q.X., Liu, B.Z., Deng, H.J., Wu, G.C., Deng, K., Chen, Y.K., Liao, P., Qiu, J.F., Lin, Y., Cai, X.F., et al. (2020). Antibody responses to SARS-CoV-2 in patients with COVID-19. Nat Med *26*, 845-848. 10.1038/s41591-020-0897-1.

Marcotte, H., Piralla, A., Zuo, F., Du, L., Cassaniti, I., Wan, H., Kumagai-Braesh, M., Andrell, J., Percivalle, E., Sammartino, J.C., et al. (2022). Immunity to SARS-CoV-2 up to 15 months after infection. iScience *25*, 103743. 10.1016/j.isci.2022.103743.

Martin-Gayo, E., Cronin, J., Hickman, T., Ouyang, Z., Lindqvist, M., Kolb, K.E., Schulze Zur Wiesch, J., Cubas, R., Porichis, F., Shalek, A.K., et al. (2017). Circulating CXCR5(+)CXCR3(+)PD-1(lo) Tfh-like cells in HIV-1 controllers with neutralizing antibody breadth. JCI Insight *2*, e89574. 10.1172/jci.insight.89574.

McMenamin, M.E., Nealon, J., Lin, Y., Wong, J.Y., Cheung, J.K., Lau, E.H.Y., Wu, P., Leung, G.M., and Cowling, B.J. (2022). Vaccine effectiveness of one, two, and three doses of BNT162b2 and CoronaVac against COVID-19 in Hong Kong: a population-based observational study. Lancet Infect Dis. 10.1016/S1473-3099(22)00345-0.

Meckiff, B.J., Ramirez-Suastegui, C., Fajardo, V., Chee, S.J., Kusnadi, A., Simon, H., Eschweiler, S., Grifoni, A., Pelosi, E., Weiskopf, D., et al. (2020). Imbalance of Regulatory and Cytotoxic SARS-CoV-2-Reactive CD4(+) T Cells in COVID-19. Cell *183*, 1340-1353 e1316. 10.1016/j.cell.2020.10.001.

Morita, R., Schmitt, N., Bentebibel, S.E., Ranganathan, R., Bourdery, L., Zurawski, G., Foucat, E., Dullaers, M., Oh, S., Sabzghabaei, N., et al. (2011). Human blood CXCR5(+)CD4(+) T cells are counterparts of T follicular cells and contain specific subsets that differentially support antibody secretion. Immunity *34*, 108-121. 10.1016/j.immuni.2010.12.012.

Mudd, P.A., Minervina, A.A., Pogorelyy, M.V., Turner, J.S., Kim, W., Kalaidina, E., Petersen, J., Schmitz, A.J., Lei, T., Haile, A., et al. (2022). SARS-CoV-2 mRNA vaccination elicits a robust and

persistent T follicular helper cell response in humans. Cell *185*, 603-613 e615. 10.1016/j.cell.2021.12.026.

Niessl, J., Baxter, A.E., Morou, A., Brunet-Ratnasingham, E., Sannier, G., Gendron-Lepage, G., Richard, J., Delgado, G.G., Brassard, N., Turcotte, I., et al. (2020). Persistent expansion and Th1-like skewing of HIV-specific circulating T follicular helper cells during antiretroviral therapy. EBioMedicine *54*, 102727. 10.1016/j.ebiom.2020.102727.

Nurieva, R.I., Chung, Y., Martinez, G.J., Yang, X.O., Tanaka, S., Matskevitch, T.D., Wang, Y.H., and Dong, C. (2009). Bcl6 mediates the development of T follicular helper cells. Science *325*, 1001-1005. 10.1126/science.1176676.

Painter, M.M., Mathew, D., Goel, R.R., Apostolidis, S.A., Pattekar, A., Kuthuru, O., Baxter, A.E., Herati, R.S., Oldridge, D.A., Gouma, S., et al. (2021). Rapid induction of antigen-specific CD4(+) T cells is associated with coordinated humoral and cellular immunity to SARS-CoV-2 mRNA vaccination. Immunity *54*, 2133-2142 e2133. 10.1016/j.immuni.2021.08.001.

Peng, Y., Mentzer, A.J., Liu, G., Yao, X., Yin, Z., Dong, D., Dejnirattisai, W., Rostron, T., Supasa, P., Liu, C., et al. (2020). Broad and strong memory CD4(+) and CD8(+) T cells induced by SARS-CoV-2 in UK convalescent individuals following COVID-19. Nat Immunol *21*, 1336-1345. 10.1038/s41590-020-0782-6.

Poon, M.M.L., Rybkina, K., Kato, Y., Kubota, M., Matsumoto, R., Bloom, N.I., Zhang, Z., Hastie, K.M., Grifoni, A., Weiskopf, D., et al. (2021). SARS-CoV-2 infection generates tissue-localized immunological memory in humans. Sci Immunol *6*, eabl9105. 10.1126/sciimmunol.abl9105.

Reynolds, C.J., Swadling, L., Gibbons, J.M., Pade, C., Jensen, M.P., Diniz, M.O., Schmidt, N.M., Butler, D.K., Amin, O.E., Bailey, S.N.L., et al. (2020). Discordant neutralizing antibody and T cell responses in asymptomatic and mild SARS-CoV-2 infection. Sci Immunol *5*. 10.1126/sciimmunol.abf3698.

Rodda, L.B., Netland, J., Shehata, L., Pruner, K.B., Morawski, P.A., Thouvenel, C.D., Takehara, K.K., Eggenberger, J., Hemann, E.A., Waterman, H.R., et al. (2021). Functional SARS-CoV-2-Specific Immune Memory Persists after Mild COVID-19. Cell *184*, 169-183 e117. 10.1016/j.cell.2020.11.029.

Roltgen, K., and Boyd, S.D. (2021). Antibody and B cell responses to SARS-CoV-2 infection and vaccination. Cell Host Microbe *29*, 1063-1075. 10.1016/j.chom.2021.06.009.

Roltgen, K., Nielsen, S.C.A., Silva, O., Younes, S.F., Zaslavsky, M., Costales, C., Yang, F., Wirz, O.F., Solis, D., Hoh, R.A., et al. (2022). Immune imprinting, breadth of variant recognition, and germinal center response in human SARS-CoV-2 infection and vaccination. Cell *185*, 1025-1040 e1014. 10.1016/j.cell.2022.01.018.

Rydyznski Moderbacher, C., Ramirez, S.I., Dan, J.M., Grifoni, A., Hastie, K.M., Weiskopf, D., Belanger, S., Abbott, R.K., Kim, C., Choi, J., et al. (2020). Antigen-Specific Adaptive Immunity to SARS-CoV-2 in Acute COVID-19 and Associations with Age and Disease Severity. Cell *183*, 996-1012 e1019. 10.1016/j.cell.2020.09.038.

Sahin, U., Muik, A., Vogler, I., Derhovanessian, E., Kranz, L.M., Vormehr, M., Quandt, J., Bidmon, N., Ulges, A., Baum, A., et al. (2021). BNT162b2 vaccine induces neutralizing antibodies and poly-specific T cells in humans. Nature *595*, 572-577. 10.1038/s41586-021-03653-6.

Schaerli, P., Willimann, K., Lang, A.B., Lipp, M., Loetscher, P., and Moser, B. (2000). CXC chemokine receptor 5 expression defines follicular homing T cells with B cell helper function. J Exp Med *192*, 1553-1562. 10.1084/jem.192.11.1553.

Sekine, T., Perez-Potti, A., Rivera-Ballesteros, O., Stralin, K., Gorin, J.B., Olsson, A., Llewellyn-Lacey, S., Kamal, H., Bogdanovic, G., Muschiol, S., et al. (2020). Robust T Cell Immunity in Convalescent Individuals with Asymptomatic or Mild COVID-19. Cell *183*, 158-168 e114. 10.1016/j.cell.2020.08.017.

Sterlin, D., Mathian, A., Miyara, M., Mohr, A., Anna, F., Claer, L., Quentric, P., Fadlallah, J., Devilliers, H., Ghillani, P., et al. (2021). IgA dominates the early neutralizing antibody response to SARS-CoV-2. Sci Transl Med *13*. 10.1126/scitranslmed.abd2223.

Thevarajan, I., Nguyen, T.H.O., Koutsakos, M., Druce, J., Caly, L., van de Sandt, C.E., Jia, X., Nicholson, S., Catton, M., Cowie, B., et al. (2020). Breadth of concomitant immune responses prior to patient recovery: a case report of non-severe COVID-19. Nat Med *26*, 453-455. 10.1038/s41591-020-0819-2.

Turner, J.S., Kim, W., Kalaidina, E., Goss, C.W., Rauseo, A.M., Schmitz, A.J., Hansen, L., Haile, A., Klebert, M.K., Pusic, I., et al. (2021a). SARS-CoV-2 infection induces long-lived bone marrow plasma cells in humans. Nature *595*, 421-425. 10.1038/s41586-021-03647-4.

Turner, J.S., O'Halloran, J.A., Kalaidina, E., Kim, W., Schmitz, A.J., Zhou, J.Q., Lei, T., Thapa, M., Chen, R.E., Case, J.B., et al. (2021b). SARS-CoV-2 mRNA vaccines induce persistent human germinal centre responses. Nature *596*, 109-113. 10.1038/s41586-021-03738-2.

Weiskopf, D., Schmitz, K.S., Raadsen, M.P., Grifoni, A., Okba, N.M.A., Endeman, H., van den Akker, J.P.C., Molenkamp, R., Koopmans, M.P.G., van Gorp, E.C.M., et al. (2020). Phenotype and kinetics of SARS-CoV-2-specific T cells in COVID-19 patients with acute respiratory distress syndrome. Sci Immunol *5*. 10.1126/sciimmunol.abd2071.

Woodruff, M.C., Ramonell, R.P., Nguyen, D.C., Cashman, K.S., Saini, A.S., Haddad, N.S., Ley, A.M., Kyu, S., Howell, J.C., Ozturk, T., et al. (2020). Extrafollicular B cell responses correlate with neutralizing antibodies and morbidity in COVID-19. Nat Immunol *21*, 1506-1516. 10.1038/s41590-020-00814-z.

Yang, Y., Yang, M., Peng, Y., Liang, Y., Wei, J., Xing, L., Guo, L., Li, X., Li, J., Wang, J., et al. (2022). Longitudinal analysis of antibody dynamics in COVID-19 convalescents reveals neutralizing responses up to 16 months after infection. Nat Microbiol *7*, 423-433. 10.1038/s41564-021-01051-2.

Yu, D., Rao, S., Tsai, L.M., Lee, S.K., He, Y., Sutcliffe, E.L., Srivastava, M., Linterman, M., Zheng, L., Simpson, N., et al. (2009). The transcriptional repressor Bcl-6 directs T follicular helper cell lineage commitment. Immunity *31*, 457-468. 10.1016/j.immuni.2009.07.002.

Zhang, J., Liu, W., Wen, B., Xie, T., Tang, P., Hu, Y., Huang, L., Jin, K., Zhang, P., Liu, Z., et al. (2019). Circulating CXCR3(+) Tfh cells positively correlate with neutralizing antibody responses in HCV-infected patients. Sci Rep *9*, 10090. 10.1038/s41598-019-46533-w.

Zhang, J., Wu, Q., Liu, Z., Wang, Q., Wu, J., Hu, Y., Bai, T., Xie, T., Huang, M., Wu, T., et al. (2021). Spike-specific circulating T follicular helper cell and cross-neutralizing antibody responses in COVID-19-convalescent individuals. Nat Microbiol *6*, 51-58. 10.1038/s41564-020-00824-5.

Zhou, P., Yang, X.L., Wang, X.G., Hu, B., Zhang, L., Zhang, W., Si, H.R., Zhu, Y., Li, B., Huang, C.L., et al. (2020). A pneumonia outbreak associated with a new coronavirus of probable bat origin. Nature *579*, 270-273. 10.1038/s41586-020-2012-7.

Zhou, Z.H., Dharmarajan, S., Lehtimaki, M., Kirshner, S.L., and Kozlowski, S. (2021). Early antibody responses associated with survival in COVID19 patients. PLoS Pathog *17*, e1009766. 10.1371/journal.ppat.1009766.

Zhu, N., Zhang, D., Wang, W., Li, X., Yang, B., Song, J., Zhao, X., Huang, B., Shi, W., Lu, R., et al. (2020). A Novel Coronavirus from Patients with Pneumonia in China, 2019. N Engl J Med *382*, 727-733. 10.1056/NEJMoa2001017.

Acknowledgements

We thank all of the participants. This work was supported by the National Natural Science Foundation of China (82061138020, 82102365), Natural Science Foundation of Hunan Province of China (2021JJ40006, 2022JJ30095), Educational Commission of Hunan Province of China (21A0529), Key Research and Development Project of Chenzhou City, Hunan Province (ZDYF2020010, ZDYF2020007, zdyf201920, zdyf201921), Key Project of The First People's Hospital of Chenzhou (N2019-002) and SC1-PHE-CORONAVIRUS-2020: "Advancing knowledge for the clinical and public health response to the 2019-nCoV epidemic" from the European Commission (CORONADX, no. 101003562) (Y.-P.L).

Author contributions

X.Q., W. L, Y.-P.L. and Y.W. contributed to the study design and data interpretation. Q.W., Q.J.W., T.X. and T.B. contributed to patient recruitment and sample collection and processing. Z.L., Y.H., J.C. and J.Y. contributed to the serum antibody binding and avidity experiments. F.C., Y.L. and S.T. contributed to pseudotyped virus production and antibody neutralization experiments. J. Z, X.Z., B.L. and B.W. contributed to all T_{FH} experiments and data analysis. X.Q., J.Z., R.H., B.L. and X.Z. drafted the manuscript. X.Q., W.L. and Y.-P.L., V.T. and Y.W. contributed to critical revision of the manuscript for important intellectual content. X.Q., W.L. and Y.-P.L. provided supervision. All authors met authorship criteria and approved the publication.

Competing interests

The authors declare no competing interests.

Figure Legends

Figure 1. Longitudinal analysis of T_{FH} cell responses in COVID-19 convalescents

(A) Diagram of sample collection from COVID-19 convalescents. The median (interquartile range, IQR) of days of sampling and the number of samples are shown for each time point. PBMCs were isolated from each blood sample for later analysis. (B) Representative flow plots of spike-specific T_{FH} cells ($CD154^{+}$) upon BSA or spike protein stimulation. (C) Spike-specific T_{FH} cells at the 2^{nd} month (n=20), 5^{th} month (n=18), 8^{th} month (n=20), 12^{th} month (n=20), and 24^{th} month (n=5), as well as healthy controls (n=17). A paired t test was used to analyse the difference between BSA and spike protein stimulation. (D) Kinetics of spike-specific T_{FH} cell responses and the stimulation index (SI). One-way analysis of variance was used to compare the differences among multiple groups, and Tukey's multiple-comparisons test was used to compare differences within the groups. The data are presented as the median ± IQR (25%–75%). $P<0.05$ was considered to be a two-tailed significant difference, ns means not significant.

Figure 2. Distinct responses of spike-specific $CXCR3^{+}$ and $CXCR3^{-}$ T_{FH} cell subsets

(A-B) Spike-specific $CXCR3^{+}$ and $CXCR3^{-}$ T_{FH} cell responses at the 2^{nd} month (n=20), 5^{th} month (n=18), 8^{th} month (n=20), 12^{th} month (n=20) and 24^{th} month (n=5) upon BSA or spike protein stimulation. A paired t test was used to analyse the difference in BSA and spike protein stimulation. (C) Kinetics of spike-specific $CXCR3^{+}$ and $CXCR3^{-}$ T_{FH} cell responses and stimulation index (SI). One-way analysis of variance was used to

compare the differences among multiple groups, and Tukey's multiple-comparisons test was used to compare differences within the groups. Data are the median ± IQR (25%–75%). (D) Comparison of spike-specific $CXCR3^+$ and $CXCR3^-$ T_{FH} cell frequency and SI. A paired t test was used to analyse the difference between $CXCR3^+$ and $CXCR3^-$ T_{FH} cell frequency or SI with BSA and spike protein stimulation. * $P<0.05$; ** $P<0.01$; *** $P<0.001$; **** $P<0.0001$. $P<0.05$ was considered to be a two-tailed significant difference, ns means not significant.

Figure 3. Kinetics of spike-specific antibody responses in COVID-19 convalescents

(A) Endpoint titers and (B) avidity index of plasma spike-specific IgG, IgG1 IgG3, and IgA antibodies in COVID-19 convalescent patients at the 2^{nd} month (n=25), 5^{th} month (n=25), 8^{th} month (n=25), 12^{th} month (n=24), and 24^{th} month (n=5) after illness onset. The endpoint titer and avidity index data were logarithmically transformed. (C) Neutralization titers of COVID-19 convalescent against SARS-CoV-2 pseudotyped virus at the indicated time points. In A, B, and C, one-way analysis of variance was used to compare the differences among multiple groups, and Tukey's multiple-comparisons test was used to compare differences within groups. Data are presented as the median ± IQR (25%–75%). (D) Correlations of spike-specific $PD\text{-}1^+$ T_{FH}, spike-specific $PD\text{-}1^+$ $CXCR3^+$ and $PD\text{-}1^+$ $CXCR3^-$ T_{FH} cells with IgG1 endpoint titers at the 5^{th} month. Spearman's rank correlation coefficient was used to describe the association between the frequencies of T_{FH} cells and subsets with the IgG1 endpoint titers. $P<0.05$ was considered a significant difference in a two-sided test.

Figure 4. The kinetics of spike-specific antibody and circulating T_{FH} cell responses in inactivated vaccine recipients

(A) Strategic diagram of vaccination and bleeding. (B) Neutralizing antibody titers against pseudotyped SARS-CoV-2 spike virus at the indicated time points ([Day 14, n=26; Day 28, n=26; Day 45, n=26; Day 90, n=25; Day 180, n=25]). Data are the mean±SEM. (C) The kinetics of spike-specific IgG avidity at different time points ([Day 14, n=26; Day 28, n=26; Day 45, n=26; Day 90, n=25; Day 180, n=25]). Data are the mean±SEM. (D) Frequencies of spike-specific T_{FH} cells and $CXCR3^+$ and $CXCR3^-$ T_{FH} cells before (Day 0, n=24) and after vaccination (Day 14, n=24; Day 28, n=23; Day 45, n=24; Day 90, n=26; Day 180, n=19). A paired t test was used to analyse the difference between T_{FH} cells and subsets between BSA and spike protein stimulation at the indicated time points, and the data are the mean±SEM. (E) Comparison of spike-specific $CXCR3^+$ and $CXCR3^-$ T_{FH} cell responses as well as the SI at the indicated time points upon BSA or spike protein stimulation. A paired t test was used to analyse the difference between $CXCR3^+$ and $CXCR3^-$ T_{FH} cells at the indicated time points, and the data are the mean±SEM. (F) Correlation between the ratio of spike-specific $CXCR3^+/CXCR3^-$ T_{FH} cells on Day 14 with neutralization antibody on Day 45 (n=24). Spearman's rank coefficient of correlation was used for T_{FH} cell and neutralization antibody analysis. * $P<0.05$; ** $P<0.01$; *** $P<0.001$; **** $P<0.0001$. $P<0.05$ was considered to be a two-tailed significant difference, ns means not significant.

Figure 5. The third dose booster promoted spike-specific antibody production and maturation

(A) Neutralization titers before and after the third dose boost (n=24), Mann□Whitney U test was used to compare the difference between two groups, data were median ± IQR (25%–75%). (B) IgG avidity before and after the third dose boost (n=24). (C) Frequencies of spike-specific T_{FH} cells and $CXCR3^+$ and $CXCR3^-$ T_{FH} cells before and after the third dose boost upon BSA or spike protein stimulation (n=24). (D) The SI of spike-specific T_{FH} cells and $CXCR3^+$ and $CXCR3^-$ T_{FH} cells before and after the third dose boost (n=24). (E) Comparison of SIs of spike-specific $CXCR3^+$ and $CXCR3^-$ T_{FH} cells before and after the third dose boost (n=24). In B-E, a paired t test was used to analyse the difference between two groups. (F) Correlation of the ratio of spike-specific $PD\text{-}1^+$ $CXCR3^+/CXCR3^-$ T_{FH} cells before the third dose and neutralization titers after the third dose boost (n=24). Spearman's rank coefficient of correlation was used for the correlation of T_{FH} cells and neutralization. $P<0.05$ was considered a significant difference in a two-sided test, ns means not significant.

Figure 6. Spike-specific $CXCR3^+$ T_{FH} cells exhibited superior capacity than spike-specific $CXCR3^-$ T_{FH} cells in supporting ASC differentiation and antibody production

(A) Diagram of the coculture of T_{FH} cells or non-T_{FH} cells with autologous memory B cells. (B) Representative flow plots of spike-specific ASCs after coculture of T_{FH} cells or non-T_{FH} cells with memory B cells from healthy controls, convalescents, and vaccinees in

the presence of SEB (100 ng/mL) for 6 days. (C-E) Comparison of total ASCs, spike-specific ASCs, and spike-specific IgG in supernatant between T_{FH} and non-T_{FH} cells after coculture with autologous memory B cells from healthy controls (n=6), convalescents (n=5), and vaccinees (n=9). (F) Total ASCs, spike-specific ASCs and spike-specific IgG before (n=7) and after (n=7) the third dose boost. (G) Diagram of coculture of $CXCR3^+$ or $CXCR3^-$ T_{FH} cells with autologous memory B cells. (H) Representative flow plots of spike-specific ASCs after coculture of $CXCR3^+$ or $CXCR3^-$ T_{FH} cells with memory B cells from convalescents and vaccinees in the presence of SEB (100 ng/mL) for 6 days. (I-J) Comparison of total ASCs, spike-specific ASCs, and spike-specific IgG in the supernatant between $CXCR3^+$ T_{FH} cells and $CXCR3^-$ T_{FH} cells after coculture with memory B cells from convalescents (n=9) and vaccinees (n=7) in the presence of SEB (100 ng/mL) for 6 days. In C-F and I-J, a paired t test was used to analyse the difference between two groups. $P<0.05$ was considered to be a two-tailed significant difference, ns means not significant.

Supporting Figure Legends

Supporting Figure 1. Gating strategy of spike-specific T_{FH} and non-T_{FH} cells

Gating strategy of spike-specific T_{FH} cells ($CD154^+$ $CXCR5^+$ $CD4^+$ T cells), spike-specific $CXCR3^+$ T_{FH} cells ($CD154^+$ $CXCR3^+$ $CXCR5^+$ $CD4^+$ T cells), spike-specific $CXCR3^-$ T_{FH} cells ($CD154^+$ $CXCR3^-$ $CXCR5^+$ $CD4^+$ T cells), active T_{FH} cells ($CD154^+$ $PD\text{-}1^+$ $CXCR5^+$ $CD4^+$ T cells), and non-T_{FH} cells ($CD154^+$ $CXCR5^-$ $CD4^+$ T cells).

Supporting Figure 2. Longitudinal analysis of non-T_{FH} cell responses in COVID-19 convalescents

(A) The frequencies of spike-specific non-T_{FH} cells at the 2^{nd} month (n=20), 5^{th} month (n=18), 8^{th} month (n=20), 12^{th} month (n=20), and 24^{th} month (n=5) after COVID-19 illness onset, as well as healthy controls (n=17) upon BSA or spike protein stimulation. A paired t test was used to analyse the difference in BSA and spike protein stimulation. (B) Kinetics of spike-specific non-T_{FH} cell responses upon BSA or spike protein stimulation and SI at the indicated time points. One-way analysis of variance was used to compare the differences among multiple groups, and Tukey's multiple-comparisons test was used to compare differences within groups. The data are presented as the median ± IQR (25%–75%). $P<0.05$ was considered to be a two-tailed significant difference, ns means not significant.

Supporting Figure 3. Differential responsiveness of spike-specific $PD\text{-}1^+$ $CXCR3^+$ and $PD\text{-}1^+$ $CXCR3^-$ T_{FH} cells in COVID-19 convalescents

Frequencies of spike-specific PD-1$^+$ CXCR3$^+$ (A) and PD-1$^+$ CXCR3$^-$ T_{FH} cells (B) at the 2nd month (n=20), 5th month (n=18), 8th month (n=20), 12th month (n=20) and 24th month (n=5) as well as healthy controls (n=17) upon BSA or spike protein stimulation. (C) Dynamics of spike-specific PD-1$^+$ CXCR3$^+$ and PD-1$^+$ CXCR3$^-$ T_{FH} cell responses at the indicated time points, as well as the SIs of spike-specific PD-1$^+$ CXCR3$^+$ and PD-1$^+$ CXCR3$^-$ T_{FH} cells. Data are the mean±SEM. In A-C, a paired t test was used to analyse the difference between two groups. * P<0.05; ** P<0.01; *** P<0.001; *** P<0.0001. P<0.05 was considered to be a two-tailed significant difference, ns means not significant.

Supporting Figure 4. Longitudinal analysis of non-T_{FH} cell responses in COVID-19 convalescents

Frequencies of spike-specific CXCR3$^+$ (A) and CXCR3$^-$ non-T_{FH} cells (B) at the 2nd month (n=20), 5th month (n=18), 8th month (n=20), 12th month (n=20), and 24th month (n=5) as well as healthy controls (n=17) upon BSA or spike protein stimulation. A paired t test was used to analyse the difference in BSA and spike protein stimulation. (C) Dynamics of spike-specific CXCR3$^+$ and CXCR3$^-$ non-T_{FH} cells at the indicated time points upon BSA or spike protein stimulation as well as their SIs. One-way analysis of variance was used to compare the differences among multiple groups, and Tukey's multiple-comparisons test was used to compare differences within the groups. Data are presented as the median±IQR (25%–75%). (D) Comparison of spike-specific CXCR3$^+$ and CXCR3$^-$ non-T_{FH} cell responses as well as SIs at the indicated time points. Data are the mean±SEM. A paired t test was used to analyse the difference between

spike-specific $CXCR3^+$ and $CXCR3^-$ non-T_{FH} cells. * P<0.05; ** P<0.01; *** P<0.001; **** P<0.0001. $P<\square 0.05$ was considered to be a two-tailed significant difference, ns means not significant.

Supporting Figure 5. Correlations of spike-specific T_{FH} cells and non-T_{FH} cells in COVID-19 convalescents

Correlations of spike-specific T_{FH} cells and spike-specific non-T_{FH} cells (A), spike-specific $CXCR3^+$ T_{FH} cells and spike-specific $CXCR3^+$ non-T_{FH} cells (B), and spike-specific $CXCR3^-$ T_{FH} cells and spike-specific $CXCR3^-$ non-T_{FH} cells (C) in COVID-19 convalescents at the 2^{nd} month (n=20), 5^{th} month (n=18), 8^{th} month (n=20), 12^{th} month (n=20), and 24^{th} month (n=5). In A, B and C, Spearman's rank correlation coefficient was used to describe the association between spike-specific T_{FH} cells and spike-specific non-T_{FH} cells. $P<\square 0.05$ was considered to be a two-tailed significant difference.

Supporting Figure 6. Correlations of spike-specific antibody endpoint titers and neutralization titers in COVID-19 convalescents

Correlation of spike-specific IgG (A), IgG1 (B), IgG3 (C), and IgA (D) endpoint titers and neutralization in COVID-19 convalescents at the 2^{nd} month (n=25), 5^{th} month (n=25), 8^{th} month (n=25), 12^{th} month (n=24), and 24^{th} month (n=5). Spearman's rank correlation coefficient was used to describe the association between the spike-specific endpoint titer and neutralization titers. $P<\square 0.05$ was considered to be a two-tailed significant difference.

Supporting Figure 7. Correlations of spike-specific IgG1 endpoint titers and spike-specific T_{FH} cells or spike-specific non-T_{FH} cells in COVID-19 convalescents

(A-C) Correlation analysis of spike-specific IgG1 endpoint titers with spike-specific T_{FH} cells (A), spike-specific $CXCR3^+$ T_{FH} cells (B), and spike-specific $CXCR3^-$ T_{FH} cells (C) in COVID-19 convalescents at the 5^{th} month (n=18). (D-F) Correlation analysis of IgG1 endpoint titers with spike-specific non-T_{FH} cells (D), spike-specific $CXCR3^+$ non-T_{FH} cells (E), and spike-specific $CXCR3^-$ non-T_{FH} cells (F) in COVID-19 convalescents at the 5^{th} month (n=18). Spearman's rank correlation coefficient was used to describe the association between IgG1 endpoint titers and T_{FH} cell subsets or non-T_{FH} cell subsets. $P<0.05$ was considered to be a two-tailed significant difference.

Supporting Figure 8. Spike-specific PD-1^+ T_{FH} cell subset responses in inactivated vaccine recipients

(A-B) Spike-specific PD-1^+ $CXCR3^+$ T_{FH} cells (A) and PD-1^+ $CXCR3^-$ T_{FH} cell (B) responses upon spike stimulation at the indicated time points in vaccinees. (C) Comparison of spike-specific PD-1^+ $CXCR3^+$ T_{FH} cell and PD-1^+ $CXCR3^-$ T_{FH} cell responses as well as SI at the indicated time points. In A-C, a paired t test was used to analyse the differences between the two groups at the indicated times, and the data are the mean ± SEM. * $P<0.05$; ** $P<0.01$; *** $P<0.001$; **** $P<0.0001$. $P<0.05$ was considered to be a two-tailed significant difference, ns means not significant.

Supporting Figure 9. Spike-specific non-T_{FH} cell responses in inactivated vaccine recipients

Spike-specific $CXCR3^+$ non-T_{FH} cell (A) and $CXCR3^-$ non-T_{FH} cell responses (B) upon spike stimulation at the indicated time points. (C) Comparison of spike-specific $CXCR3^+$ non-T_{FH} cell and $CXCR3^-$ non-T_{FH} cell frequencies as well as SIs. In A-C, a paired t test was used to analyse the difference between two groups at the indicated times, and the data are the mean ± SEM. * P<0.05; ** P<0.01; *** P<0.001; **** P<0.0001. P< 0.05 was considered to be a two-tailed significant difference, ns means not significant.

Supporting Figure 10. A third dose boost promoted spike-specific non-T_{FH} cell responses in inactivated vaccine recipients

(A) Frequencies of spike-specific non-T_{FH} cells, spike-specific $CXCR3^+$ non-T_{FH} cells, and spike-specific $CXCR3^-$ non-T_{FH} cell responses before and 14 days after the third dose boost upon BSA or spike protein stimulation (n=24). (B) SIs of spike-specific non-T_{FH} cells, spike-$CXCR3^+$ non-T_{FH} cells, and spike-specific $CXCR3^-$ non-T_{FH} cells before and 14 days after the third dose boost (n=24). (C) Comparison of SI between spike-specific $CXCR3^+$ non-T_{FH} cells and spike-specific $CXCR3^-$ non-T_{FH} cells before and 14 days after the third dose boost (n=24). In A-C, a paired t test was used to analyse the difference between two groups. P< 0.05 was considered to be a two-tailed significant difference, ns means not significant.

Supporting Figure 11. Correlation of spike-specific ASCs with spike-specific IgG in supernatants after coculture

Correlation of spike-specific ASCs and the spike-specific IgG OD_{450} after coculture of T_{FH} cells with autologous memory B cells from convalescents (n=5) and vaccinated subjects (n=14) in the presence of SEB (100 ng/mL) for 6 days. Spearman's rank correlation coefficient was used to measure the correlation between two different variables. $P<0.05$ was considered to be a two-tailed significant difference.

Figure 1

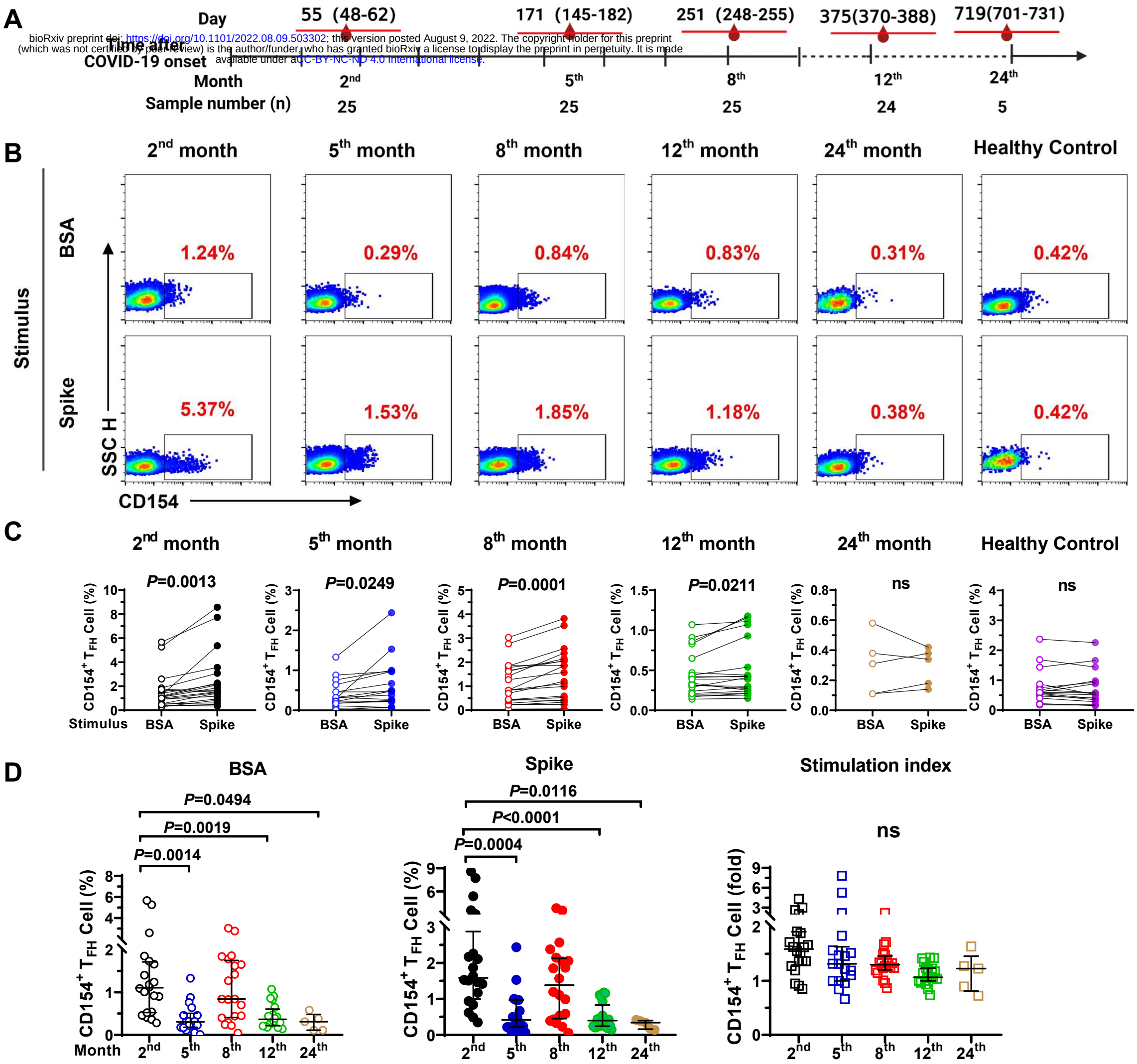

Figure 2

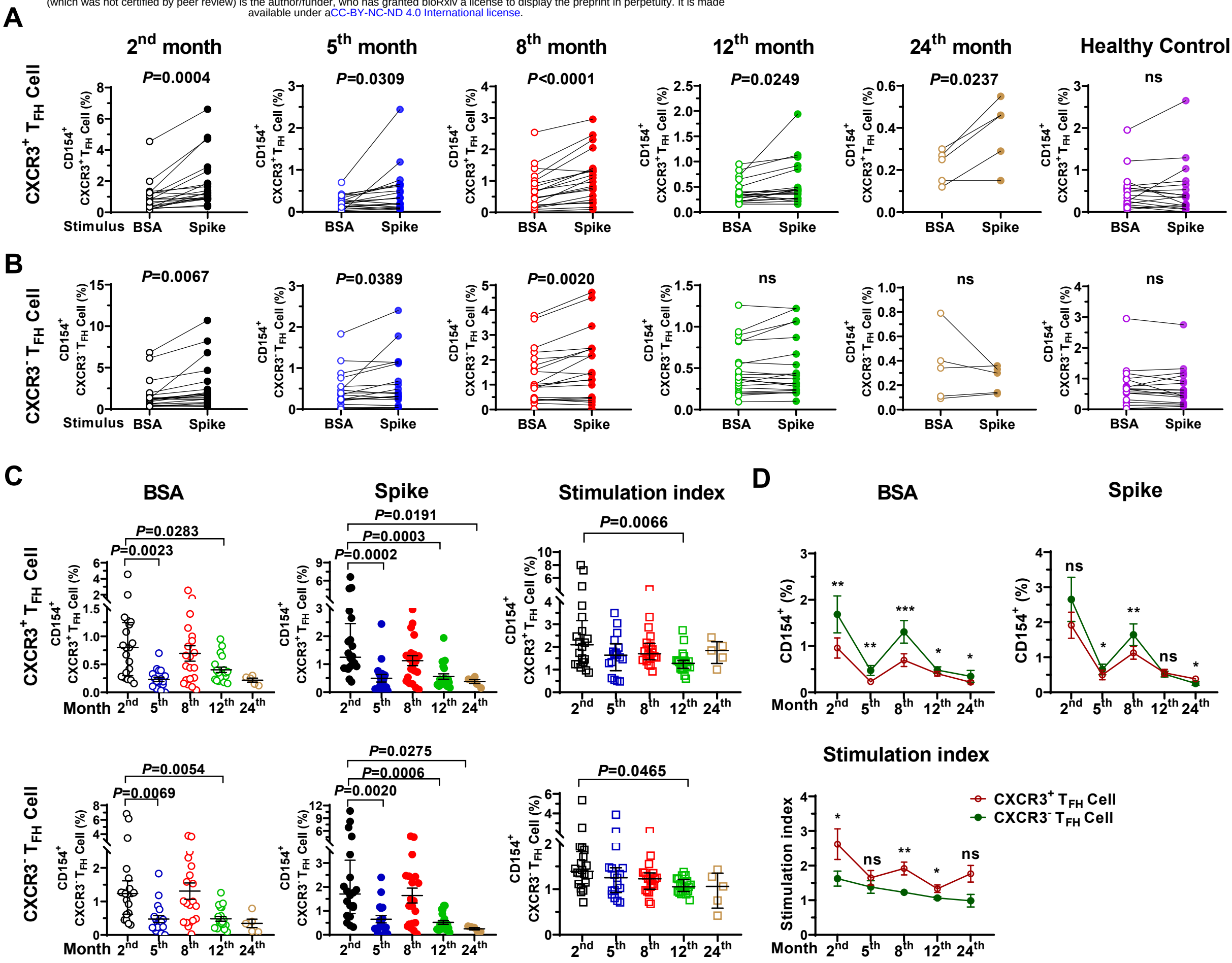

Figure 3

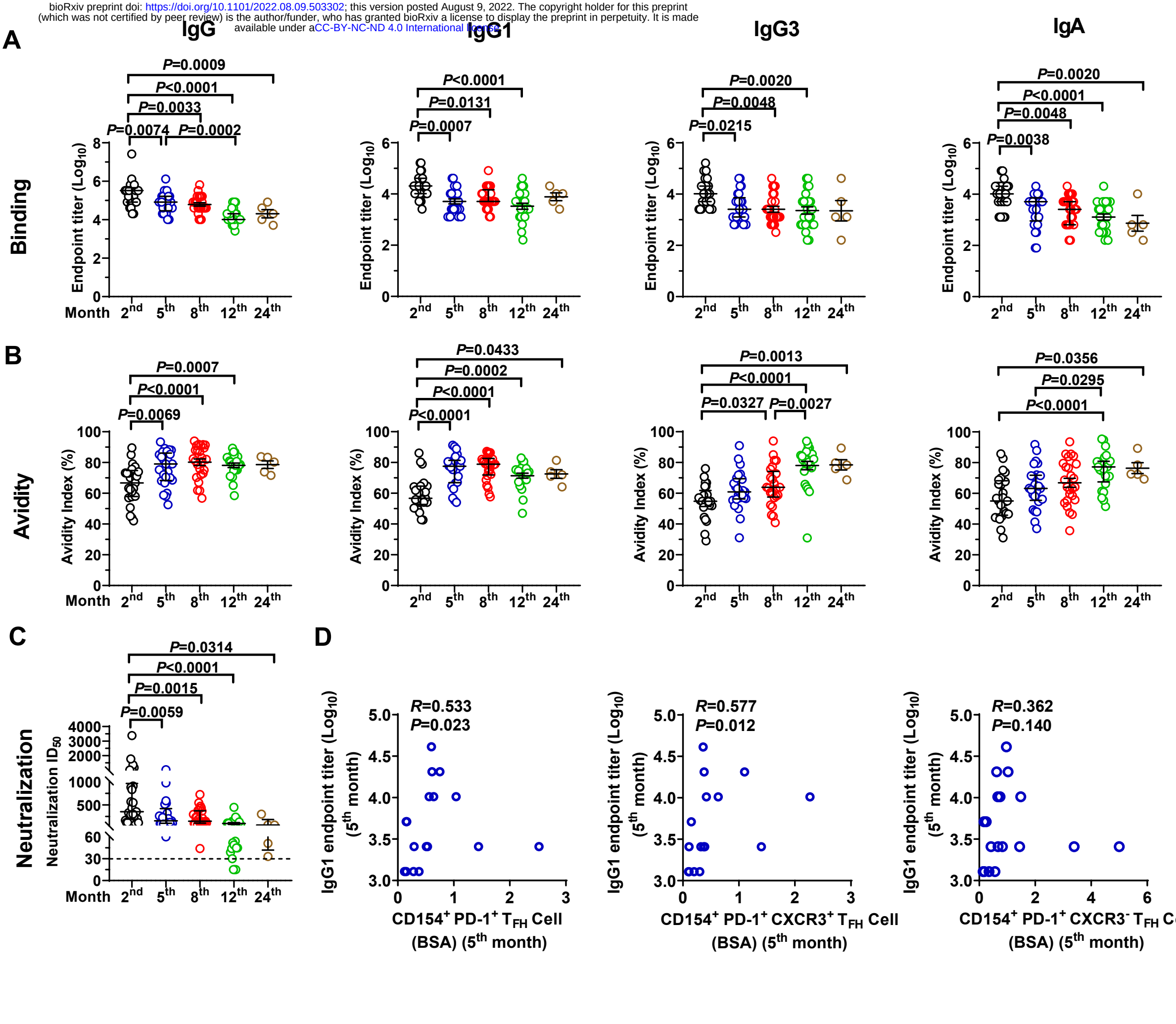

Figure 4

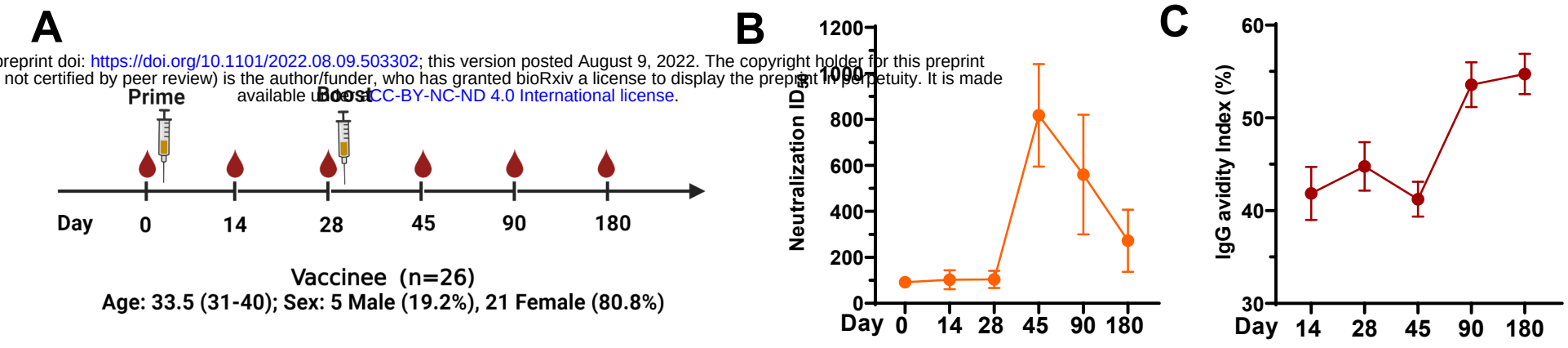

Figure 5

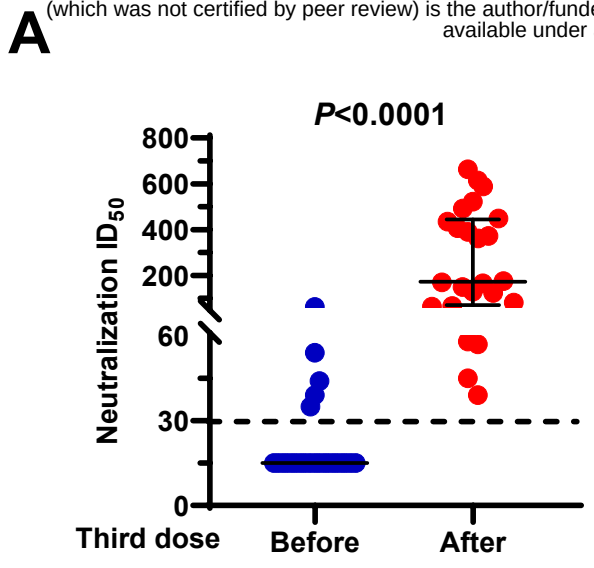

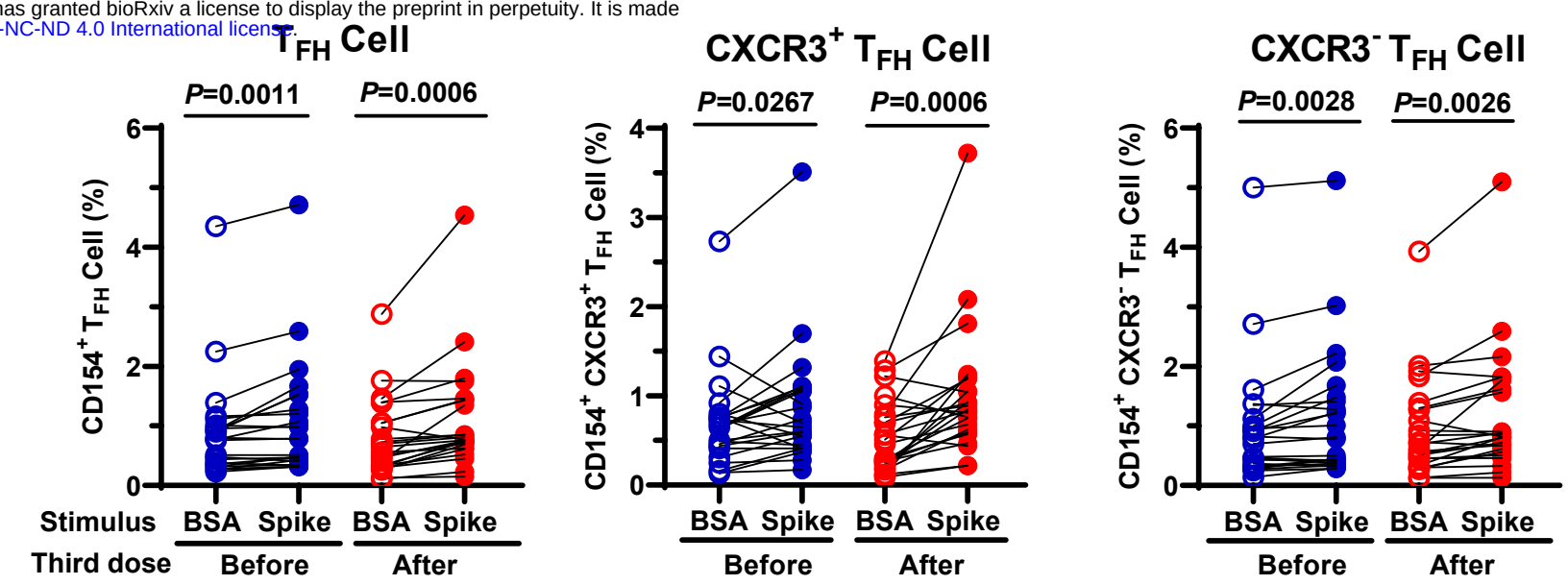

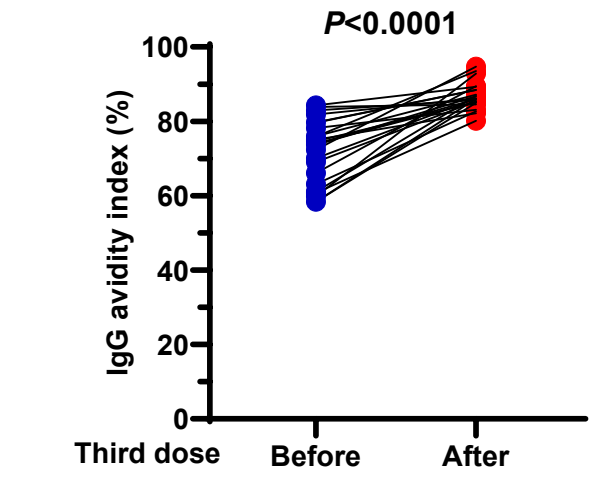

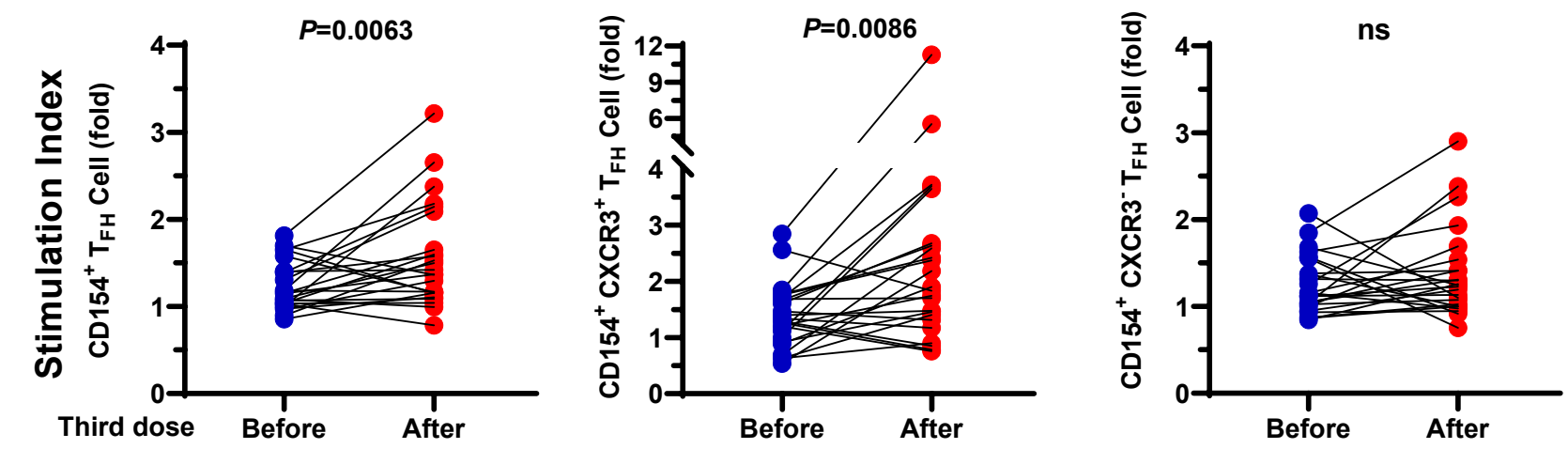

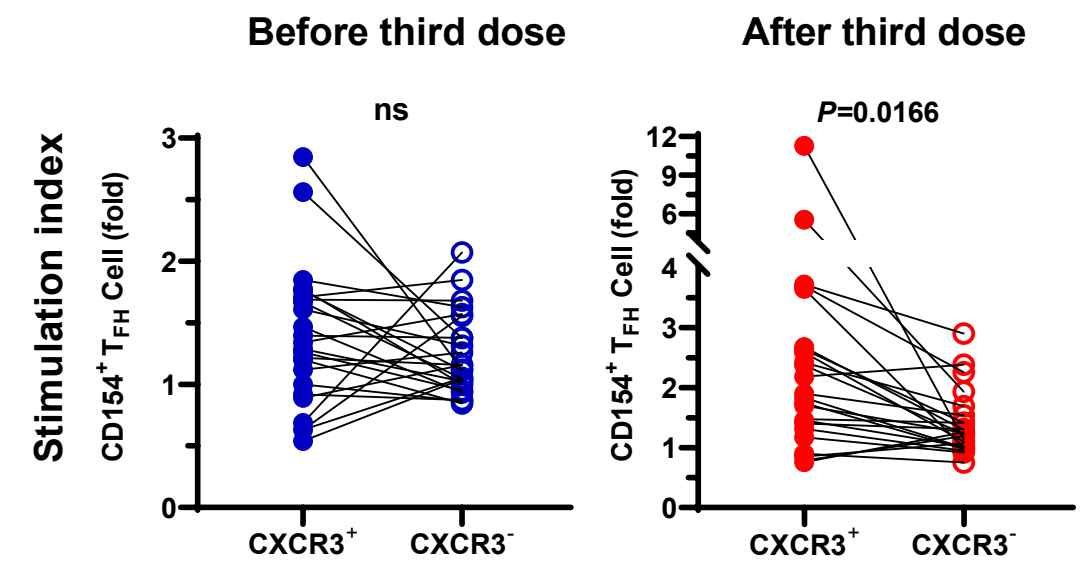

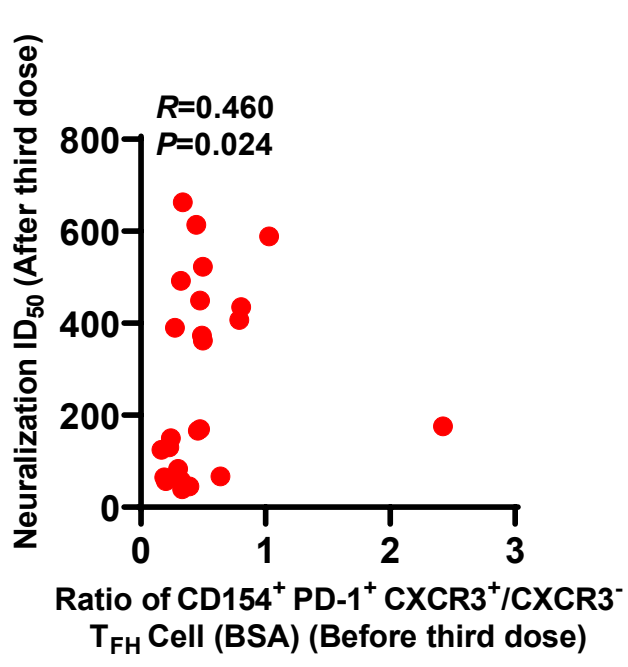

Figure 6